AD-A142 125 RESEARCH ON THE CRYSTAL GROWTH AND DIELECTRIC PROPERTIES OF HIGH PERMITTI..(U) ROCKWELL INTERNATIONAL THOUSAND OAKS CA SCIENCE CENTER R NEURGAONKAR ET AL. MAY 84 SC5345.4AR N00014-81-C-0463 1/1

UNCLASSIFIED F/G 20/2 NL

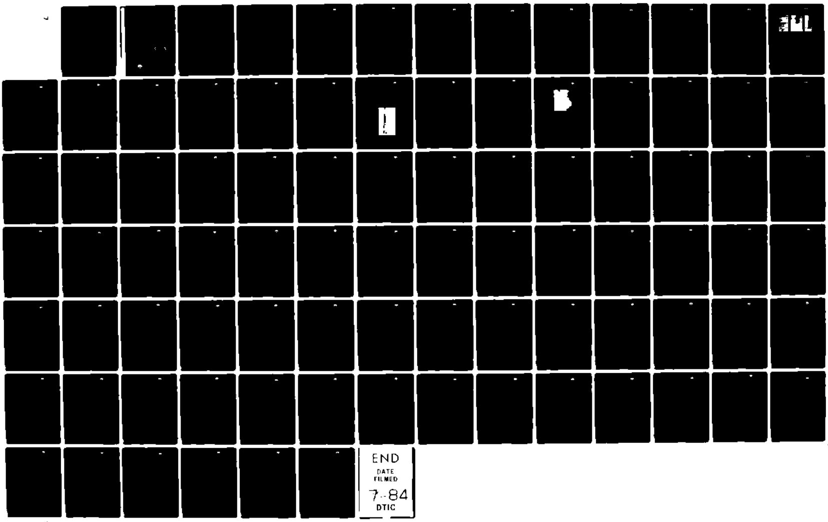

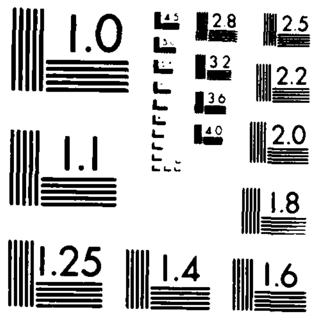

MICROCOPY RESOLUTION TEST CHART
NATIONAL BUREAU OF STANDARDS-1963-A

(12)

SC5345.4AR

Copy No. 5

SC5345.4AR

RESEARCH ON THE CRYSTAL GROWTH AND DIELECTRIC PROPERTIES OF HIGH PERMITTIVITY FERROELECTRIC MATERIALS

ANNUAL REPORT FOR THE PERIOD
March 1, 1983 through February 29, 1984

CONTRACT NO. N00014-81-C-0463
PROJECT NO. NR 032-609(471)

AD-A142 125

Prepared for

Office of Naval Research
800 North Quincy Street
Arlington, VA 22217

R.R. Neurgaonkar
Program Manager

MAY 1984

Rockwell International
Science Center

UNCLASSIFIED
SECURITY CLASSIFICATION OF THIS PAGE

REPORT DOCUMENTATION PAGE

1a. REPORT SECURITY CLASSIFICATION: Unclassified

1b. RESTRICTIVE MARKINGS:

2a. SECURITY CLASSIFICATION AUTHORITY:

2b. DECLASSIFICATION/DOWNGRADING SCHEDULE:

3. DISTRIBUTION/AVAILABILITY OF REPORT: ~~Reproduction in whole or in part is permitted for any purpose of the United States Government~~
Approved for public release; distribution unlimited.

4. PERFORMING ORGANIZATION REPORT NUMBER(S): SC5345.4AR

5. MONITORING ORGANIZATION REPORT NUMBER(S):

6a. NAME OF PERFORMING ORGANIZATION: Rockwell International Science Center

6b. OFFICE SYMBOL *(If applicable)*:

7a. NAME OF MONITORING ORGANIZATION:

6c. ADDRESS *(City, State and ZIP Code)*: 1049 Camino Dos Rios, Thousand Oaks, California 91360

7b. ADDRESS *(City, State and ZIP Code)*:

8a. NAME OF FUNDING/SPONSORING ORGANIZATION: Office of Naval Research

8b. OFFICE SYMBOL *(If applicable)*:

9. PROCUREMENT INSTRUMENT IDENTIFICATION NUMBER: Contract No. N00014-81-C-0463

8c. ADDRESS *(City, State and ZIP Code)*: 800 North Quincy Street, Arlington, VA 22217

10. SOURCE OF FUNDING NOS.

PROGRAM ELEMENT NO.	PROJECT NO.	TASK NO.	WORK UNIT NO.
	NR 032-609 (471)		

11. TITLE *(Include Security Classification)*: RESEARCH ON THE CRYSTAL GROWTH AND DIELECTRIC PROPERTIES OF HIGH PERMITTIVITY FERROELECTRIC MATERIALS (U)

12. PERSONAL AUTHOR(S): Neurgaonkar, Ratnakar; Oliver, John R.

13a. TYPE OF REPORT: Annual Report

13b. TIME COVERED: FROM 03/01/83 TO 02/29/84

14. DATE OF REPORT *(Yr., Mo., Day)*: MAY 1984

15. PAGE COUNT: 87

16. SUPPLEMENTARY NOTATION:

17. COSATI CODES

FIELD	GROUP	SUB. GR.

18. SUBJECT TERMS *(Continue on reverse if necessary and identify by block number)*: Tungsten Bronze, SBN, BSKNN, KLN, PBN, Millimeter Wave, Striations, Temperature Dependence, Electro-optic Coefficient.

19. ABSTRACT *(Continue on reverse if necessary and identify by block number)* SBN & BSKNN

Millimeter wave measurements on tungsten bronze $Sr_{1-x}Ba_xNb_2O_6$ (SBN) and $Ba_{1-2x}Sr_xK_{1-y}Na_yNb_5O_{15}$ (BSKNN) have shown a strong temperature dependence for the permittivity and dielectric losses, with both decreasing at low temperatures down to 77K for the electric field parallel to the polar axis. The observed changes in ϵ' and ϵ'' perpendicular to the polar axis are much less, being only 30–40%. A temperature sensitive peak in the polar ϵ'' has been observed for some samples.

SBN crystals doped with Ce and Fe and have been successfully grown under DARPA contract, and work is continuing on improvements in the overall crystal quality of this bronze. Work is also continuing on the growth of ceramic and single crystal BSKNN, and ceramic KLN for evaluation of the millimeter wave properties of large unit cell "stuffed" bronzes. Grain oriented, hot-pressed $Pb_{1-x}Ba_xNb_2O_6$ (PBN) is also being developed in order to examine the properties of morphotropic phase boundary bronze compositions.

20. DISTRIBUTION/AVAILABILITY OF ABSTRACT: UNCLASSIFIED/UNLIMITED ☒ SAME AS RPT. ☐ DTIC USERS ☐

21. ABSTRACT SECURITY CLASSIFICATION: Unclassified

22a. NAME OF RESPONSIBLE INDIVIDUAL:

22b. TELEPHONE NUMBER *(Include Area Code)*:

22c. OFFICE SYMBOL:

DD FORM 1473, 83 APR — EDITION OF 1 JAN 73 IS OBSOLETE.

UNCLASSIFIED
SECURITY CLASSIFICATION OF THIS PAGE

TABLE OF CONTENTS

LIST OF TABLES

LIST OF FIGURES

LIST OF FIGURES

1.0 INTRODUCTION AND PROGRESS SUMMARY

High permittivity ferroelectric materials such as the tungsten bronzes and perovskites have shown substantial promise for the manipulation of interactions involving electric fields at frequencies from dc to the infrared. In the last few years, interest has grown in millimeter wave applications for communications and target-seeking radars, and there has developed a need to characterize the linear and nonlinear dielectric properties of ferroelectrics in this new frequency range.

The research effort reported on herein is part of a long-range program whose objective is to determine the range of dielectric properties attainable at millimeter wave frequencies in various classes of high permittivity ferroelectrics, and to relate these properties to fundamental crystal characteristics. This work involves the preparation of new ferroelectrics in single crystal and ceramic form, characterization of their crystal structure and low frequency dielectric response, and measurement of both linear and nonlinear dielectric properties at millimeter wave frequencies.

Much of the early effort in this program was devoted to single crystal strontium barium niobate (SBN), a tunsten bronze with unusually large room-temperature dielectric response. More recently, other tungsten bronzes such as potassium lithium niobate (KLN) and barium strontium potassium sodium niobate (BSKNN) have been prepared and studied to elucidate the role of unfilled crystallographic sites in influencing dielectric loss. Currently, we are developing preparation techniques for an unusual bronze, lead barium niobate (PBN), which should exhibit exceptionally large nonlinear electrical and optical response for a Pb:Ba ratio of 60:40, where it undergoes a transition from tetragonal to orthorhombic form.

Millimeter wave characterization of these materials has revealed two related, but unexpected, features: the polar axis permittivity at room temperature shows large dispersion, and the polar axis dielectric loss is very large, with tan δ approaching unity in some cases. The frequency dependence does not fit a classic relaxor or softmode form, even allowing for a frequency dependent relaxation rate.

Following up an observation due to Fetterman,[1] we have recently begun a study of low-temperature effects on the dielectric properties of these materials. Cooling to liquid nitrogen temperature is found to drastically reduce the loss along the polar axis in both SBN and BSKNN. This strongly implicates phonon population as a controlling factor in the room-temperature loss. However, dielectric properties perpendicular to the polar axis are only marginally affected. There are other unusual features of the temperature dependence which, taken together, indicate that a suitable explanation for the observed properties will be difficult to construct. It is our present view that a systematic study of these features will allow many of the underlying mechanisms controlling the microwave dielectric response to be identified.

2.0 MILLIMETER WAVE APPLICATIONS

The inherent advantages of millimeter wave radar systems in terms of all-weather capability when compared to infrared and optical sensors, and reduced weight and size when compared to conventional microwave radars, have led to increased emphasis by defense agencies on the development of millimeter wave seekers for a broad spectrum of major weapons systems. Device requirements for such radar systems were recently identified at an ARO-sponsored workshop on Short Millimeter Wave Non-Reciprocal Materials and Devices. It was concluded that while considerable advances have been made in the areas of sources of radiation, mixers, detectors, and receivers, there is a lack of comparable progress in the areas of components such as reciprocal and non-reciprocal devices (e.g., phase shifters, isolators, and circulators) and electronic-scanning antennas. It was recognized that new device concepts should be explored, and better materials developed (ferroelectric, ferrimagnetic, and semiconducting) to support these concepts.

One concept which we have been investigating is phase shifting by means of the large nonlinear susceptibility of ferroelectric materials. Sensitivities (dn/dE) of the millimeter wave refractive index approaching 10^{-4} meters/volt are predicted for simple proper ferroelectrics from Devonshire models for the dielectric properties. Such materials can be used either as single discrete phase-shifting components in waveguides or as planar dielectric lenses. In the latter case, linear variation of the applied electric field across the lens will produce a uniform deflection of the millimeter wave beam passing through the lens, permitting electronic scanning of the beam. In either case, losses in passing through the phase-shifting material must be kept low ($\sim$ 1 dB) and the magnitude of applied voltages should fall within an accessible range for small, lightweight systems.

3.0 CURRENT PROGRESS

3.1 Single Crystal Growth of SBN

The system $Sr_{1-x}Ba_xNb_2O_6$ (SBN) is a tetragonal tungsten bronze with a point group symmetry 4 mm. We have been extensively involved in the development of the Czochralski crystal growth technology for this important bronze for several years with excellent success in the growth of large diameter (1 - 2 cm) crystals. Recently the growth technology has undergone some modification in order to improve overall crystal quality, particulary with regard to optical defects and striations. Since SBN:60 is reported to be the only congruent melting composition in $SrNb_2O_6$-$BaNb_2O_6$ system,[2] the current effort, under DARPA contract, has mainly concentrated on this composition.

It is now well established that there are several factors that influence the quality and size of bronze crystals. The present improvements in SBN crystal quality and size have resulted from the following changes in the growth technique:

- Use of higher purity starting materials to eliminate striations caused by impurity ions, i.e., Ca^{2+} and Na^{+}.
- Eliminated the use of iridium crucible: no iridium contamination.
- Established pulling and rotation rates for SBN:60 crystals.
- Effectively implemented an automatic diameter control (ADC) system to minimize temperature instability during growth.

The adaptation of the ADC system is the most recent modification of our Czochralski growth technology. The need for automativc diameter control in growing SBN single crystals arises mainly from the poor thermal conductivity of the material, which causes great difficulty in maintaining a fixed crystal diameter by set-point programming of the furnace power. It has been noticed that small changes on the order of ± 1° to 2° in the thermal environment near the growing interface tend to continually upset the steady-state heat flow through the crystal, either increasing it to cause crystal widening or decreasing it to cause crystal narrowing. Uniform crystal diameter implies unchanging melt temperature near the interface, a necessary and important ingredient for producing homogeneous, striae-free crystals.

A crucible-weighing ADC system has been installed for this task, since the technology is well established and good equipment is commercially available. The ADC system has been modified in the current arrangement, with some furnace redesign necessary and electronically matched to the growth furnace thermal time constant to achieve the smoothest possible changes in furnace power in order to hold the growth interface conditions as steady as possible. This has been accomplished over a period of many experiments.

SBN:60 crystals grown using the automatic diameter control system are exceptionally uniform with optical striations being greatly minimized or totally absent. As shown in Fig. 1, the striae pattern of SBN:60 crystals sectioned and polished parallel to the growth axis [001] clearly show that the growth under rapidly changing thermal conditions (left) contains strong striae, then a transition zone occurs (center) as the crystal begins to achieve constant diameter. In this section, striae tend to be weak. ADC is engaged during at this point and, as growth continues, the system settles down to constant diameter growth with striae absent, or nearly so (extreme right). This is a significant accomplishment, and it shows that the ADC system can be effectively used to maintain uniform crystal diameter and thereby reduce or eliminate striations and other crystal defects.

Doped SBN:60 single crystals, e.g., Ce^{3+} and Fe^{3+}, have also been grown with some success, and although the addition of dopants requies some alteration of the growth parameters, it does not appear to cause any serious or insurmountable degradation of crystal quality. Figure 2 shows the low frequency (10 kHz) dielectric behavior as a function of temperature for an Fe^{3+}-doped SBN:60 c-axis crystal. The general behavior is quite good and comparable to undoped material, but with a lower value for ε at the Curie point. The lower value for T_c of 53°C vs 72°C for undoped SBN:60 results in a significantly higher value for the low frequency dielectric constant at room temperature, being 3000 for ε_{33} after

SC83-24485

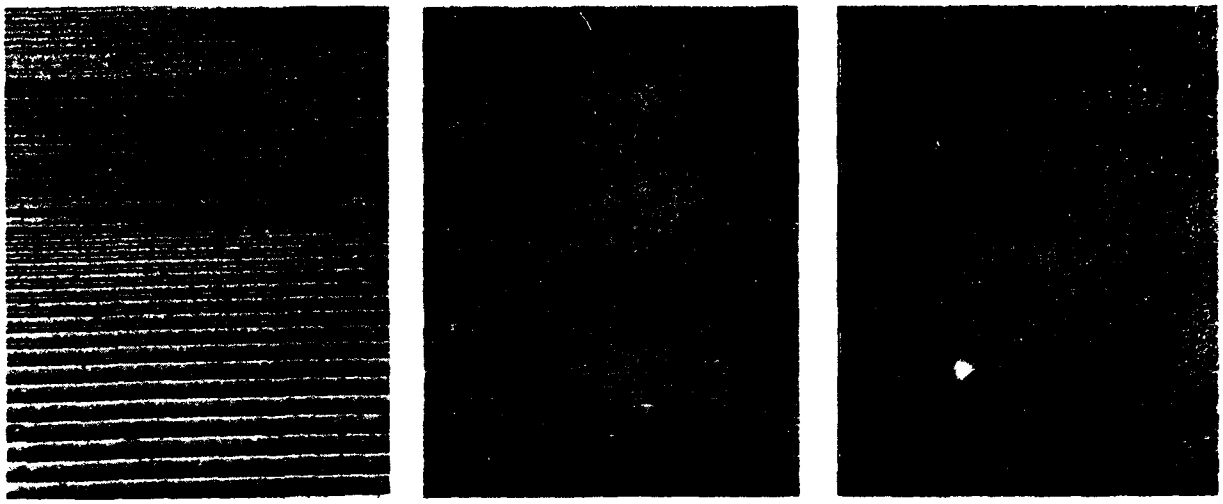

SBN:60 CRYSTAL GROWTH WITHOUT ADC SYSTEM

SBN:60 CRYSTAL GROWTH WITH ADC SYSTEM (UNSTABLE CONDITIONS)

SBN:60 CRYSTAL GROWTH WITH ADC SYSTEM AFTER ESTABLISH CONDITIONS

Fig. 1 Striation patterns for SBN:60 single crystals with and without ADC.

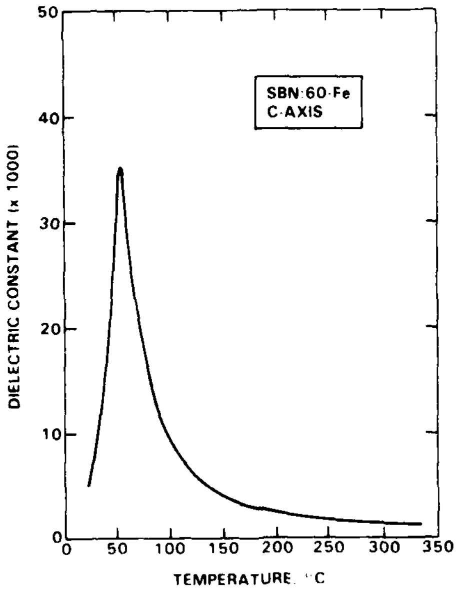

Fig. 2 10 kHz dielectric behavior of an Fe^{3+}-doped SBN:60 single crystal (c-axis).

8 kV/cm poling using the field-cooling method. Dielectric values along the a-axis are much lower, typically 470 at room temperature and unaffected by poling. Dielectric losses (tan δ) are 0.004-0.007 for all three crystallographic axes over the range of 100 Hz - 100 kHz, and are comparable to values for undoped SBN:60.

Similarly good results have been achieved with Ce^{3+}-doped SBN:60, albeit with a lower c-axis dielectric constant of 940 at room temperature. The addition of Ce^{3+} did not show any significant change in T_c over undoped material. Both Fe^{3+} and Ce^{3+}-doped SBN crystals will continue to be developed in order to achieve greater size, uniformity, and optical quality.

3.2 PBN Development

Our initial work on the tungsten bronze $Pb_{1-x}Ba_xNb_2O_6$ (PBN) has shown this material to be very promising for a number of applications, including piezoelectric, electro-optic, nonlinear optic, and acousto-optic device applications. This solid solution system possesses both orthorhombic and tetragonal forms, with a morphotropic phase boundary occurring at x = 0.37. The phase diagram for this system as a function of Ba^{2+} content has been established based on our previous work on ceramic and single crystal samples of this material, and is shown in Fig. 3. Concurrent theoretical modeling has shown an enhancement of the ferroelectric properties of PBN near the morphotropic phase boundary between the ferroelectric orthorhombic (mm2) and ferroelectric tetragonal (4 mm) structures near the composition $Pb_{0.6}Ba_{0.4}Nb_2O_6$.[3] This has been experimentally verified using small single crytals grown by the Czochralski technique.

Although we have been able to grow small to medium sized single crystals of PBN, growth is generally difficult for a number of reasons. These include loss of lead (Pb^{2+}) due to its high volatility at the melt temperature, compositional gradients in the grown crystals, and crytal cracking when cycling through the paraelectric-ferroelectric phase transition temperature. The alternative approach to this problem is the development of the hot-pressing technique which is now routinely used for perovskite PLZT and other compositions.[4-6]

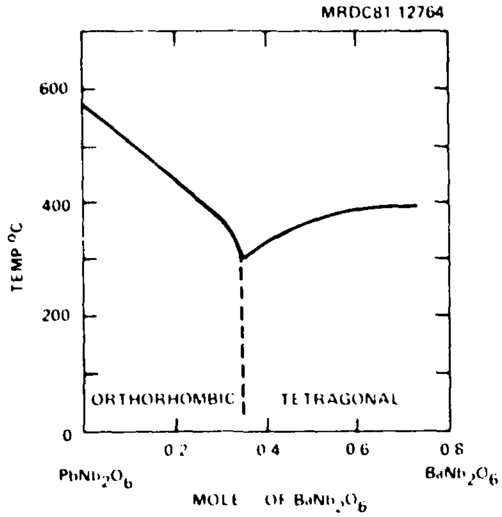

Fig. 3 Phase diagram for the bronze system $Pb_{1-x}Ba_xNb_2O_6$.

Recently Yokosuka[7] and Nagata and Okazaki[8] investigated the ferroelectric and optical properties of hot-pressed ceramic PBN, and their results are very encouraging. Because of the lower growth temperatures (~ 1300°C) necessary for hot-pressed fabrication of PBN, the problems of lead loss are significantly reduced under these conditions. Furthermore, the addition of small amounts of La in the form $(Pb_{1-x}Ba_x)_{1-3y/2}La_yNb_2O_6$ (PBLN(1-x/x/y)) has been found to significantly enhance the transparency and optical quality of the material,[8] while also reducing the Curie temperature from that of unmodified PBN. Published data for the linear and quadratic electro-optic coefficients, r_c and R_c, for hot-pressed PBLN are shown in Table 1, and are seen to be quite high for several compositions.

Hot-pressing has been used effectively for ferroelectric ceramic research and development technology since materials can easily be fabricated in a variety of sizes and shapes with good cmpositional control. Based on the studies by Land and Haertling,[5,6] the technique has proven to be successful for the densification of the perovskite PLZT compositions. Furthermore, it is interesting to note that the electro-optic as well as pyroelectric properties are improved to a degree such that electro-optic devices including displays, optical shutters, spectral filters and memories, several pyroelectric devices, and millimeter wave devices now appear feasible using ceramic materials.

Table 1
Electro-Optic Properties of La-Modified PBN Dense Ceramics

Composition*	r_c (10^{-10} m/V)	R_c (10^{-16} m^2/V^2)
60/40/2	4.42	-
60/40/3	7.45	-
60/40/4	6.66	-
70/30/2	1.72	-
60/40/8	-	2.09
60/40/10	-	1.16
70/30/8	-	1.58

Our initial hot-pressed growths of La-modified $Pb_{0.60}Ba_{0.40}Nb_2O_6$ have been highly successful. These growths have been made using graphite die sets in an N_2 atmosphere with a uniaxial pressure of 3000-4000 psi at 1240-1290°C. The resulting 1 - 2 in. diameter disks are generally crack-free and mechanically very strong. Subsequent to densification, sample slices are oxidized at 1000 - 1100°C for up to several hours, resulting in white to cream colored, translucent material.

The incorporation of La as $(Pb_{0.60}Ba_{0.40})_{1-3/y/2}La_yNb_2O_6$ (PBLN) results in an improvement in the optical quality of PBN based on Japanese work.[7,8] To date, the use of La in our PBN ceramics has been limited to 2% incorporation in order to examine the initial effects of La-modified PBN in comparison with unmodified material. Hence, the improvement in optical transmission is small in comparison with anticipated results for La modifications in the 5 - 8% range.[8] Aside from the improvement in the optical quality, La modification has three significant effects on the dielectric properties and growth of PBN. First, the Curie temperature is reduced in comparison with unmodified material. Second, the dielectric constant at the Curie point is also reduced to some extent, although the amount of reduction has not been quantitatively established with confidence due to variables in processing. Finally, the incorporation of La in

PBN significantly reduces the loss of Pb^{2+} during hot-pressed densification by a factor of 3 or more. This result is consistent with our observations of weight loss in the tungsten bronze ceramic $Pb_{1-2x}K_xLa_xNb_2O_6$ during sintering,[9] and suggests the possibility of modifying PBN with small amounts of K + La as a means of reducing Pb^{2+} loss while providing some flexibility in control over the dielectric properties.

The work by Nagata et al[8] on PBLN has shown that grain orientation is possible in hot-pressed dense ceramic growths of this material. This is confirmed in our own work, in which dielectric anisotropies greater than 1.5:1 have been observed for directions perpendicular and parallel to the pressing direction for tetragonal PBLN (60/40/2). A summary of the dielectric data for one such growth is given in Table 2. Since the substitution of Ba for Pb in $PbNb_2O_6$ first decreases the orthorhombic distortion and then induces a tetragonal structure with the polar axis along the c-axis rather than the orthorhombic b-axis, these results support the conclusion that the c-axis is oriented perpendicular to the uniaxial hot-pressing direction. This is further supported by the fact that melted powders of other tetragonal bronzes such as SBN tend to recrystallize into needle-shaped grains oriented along the c-axis.

Table 2
Dielectric Properties of Hot-Pressed PBLN (60/40/2)

	Dielectric Constant, K		Dielectric Loss at 23°C	
Orientation	@ 23°C	@ T_c*	1 KHz	100 KHz
Perpendicular-cut	2100	7440	0.0145	0.0325
Parallel-cut	1370	4060	0.0205	0.0330

*$T_c \sim 260°C$

Recently we began an investigation of the ferroelectric properties in the general ternary phase system PbO-BaO-Nb_2O_5 using sintered ceramic samples. This on-going research has revealed a number of interesting features of this system, and so far indicates that the dielectric properties are maximized along the pseudo-binary join $PbNb_2O_6$-$BaNb_2O_6$ at the morphotropic boundary between the orthorhombic and tetragonal structures. Using near-morphotropic $Pb_{0.60}Ba_{0.40}Nb_2O_6$ as the reference composition, we investigated the dielectric and structural properties of $Pb_xBa_{0.4}Nb_2O_6$, $0.5 > x > 1.0$, using normally pressed and sintered samples. Figure 4 shows that the dielectric constant at the Curie point attains a maximum at an as-prepared value of $x = 0.65$; when the nominal 10% loss of PbO during sintering is taken into account, the maximum is seen to occur at virtually the stoichiometric $Pb_{0.60}Ba_{0.40}Nb_2O_6$ composition.

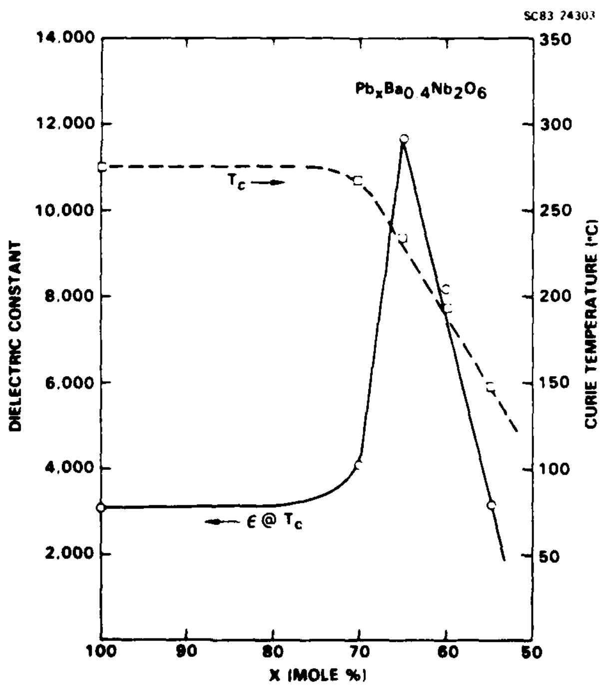

Fig. 4 Dielectric propertis and Curie temperature as a function of Pb^{2+} content for $Pb_xBa_{0.4}Nb_2O_6$.

These initial results on grain-oriented, hot-pressed dense ceramic PBLN are highly encouraging, and point the way toward further development of this material. Clearly it would be preferable to perform hot-pressed densification of this oxide ferroelectric in an oxidizing atmosphere rather than in the inert

N_2 atmosphere required by the present graphite die sets. However, this may prove to be a disadvantage in certain cases, as there is some evidence which suggests that the degree of oxidation may affect the dielectric properties of PBN/PBLN, specifically the location of the Curie point and the magnitude of dielectric losses. The effects of sintering temperature, uniaxial pressure, and cooling rate on the ionic site preference between the 12- and 15-fold coordinated lattice sites has a strong influence on the Curie temperature T_c and the dielectric properties, and to date these effects are only partially identified. Future work on La-modified PBN will focus on improvements in the hot-pressing technique in order to optimize the dielectric properties of this bronze system.

3.3 Single Crystal Growth of BSKNN and KLN

Growth of the "stuffed" bronze $Ba_{2-x}Sr_xK_{1-y}Na_yNb_5O_{15}$ (BSKNN) has continued with the composition $Ba_{1.2}Sr_{0.8}K_{0.75}Na_{0.25}Nb_5O_{15}$ using the Czochralski technique. This particular compositon is congruent melting and has shown particularly interesting potential for photorefractive applications as well as for millimeter wave device research. Crystals have been grown from platinum crucibles at 1480°C in an oxygen ambient, and recently we have been able to grow a 1.2 × 1.2 cm square cross-section boule, the largest to date.

The basic problem confronting Czochralski single crystal growth of BSKNN is one of bulk fracture during cooldown arising from induced crystal strain during growth. Automatic diameter control (ADC) is now being used to minimize this problem, but its use has been restricted to smaller boules on the order of 0.5 cm^2. Extensive modification of the crystal growth unit is now being implemented in order to reduce the temperature gradients even further and eliminate the fracture problem encountered with larger crystals.

Because of the need to investigate and better understand the millimeter wave dielectric properties of the tungsten bronzes, specifically the dielectric losses as a function of temperature, another large unit cell bronze, $K_3Li_2Nb_5O_{15}$ (KLN), has been selected for investigation. KLN is the largest unit cell bronze grown to date (a, b = 12.585Å, c = 4.015Å) and is potentially interesting in comparison with the dielectric properties of BSKNN and smaller unit cell bronzes such as SBN. Single crystals of KLN have been successfully grown by the Czochralski technique in work performed under AFOSR sponsorship.[10] In the course of this study, it was clearly observed that the rate of crystallization along the c-axis was much faster than those along any other directions; the crystals, however, cracked when grown along the c-axis. This cracking problem was nearly eliminated when the crystals were grown along the a-axis and such crystals were of excellent quality, with diameters of up to 0.5 - 0.7 cm (Fig. 5). Considerable work has been done on the Czochralski growth technique in order to obtain larger diameter (> 1 cm), crack-free KLN crystals; however, to date no such crystals have been grown without considerable fracture.

SC81-15568

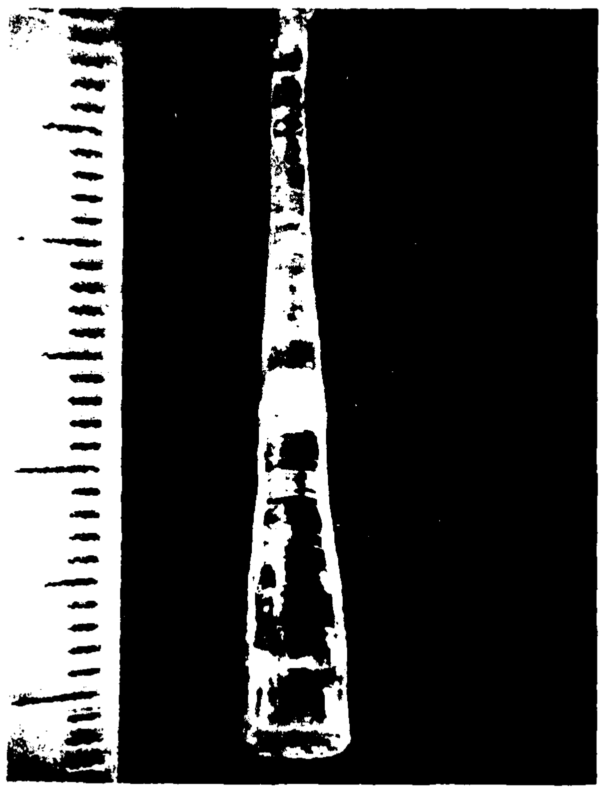

Fig. 5 Single crystal KLN grown along the a-axis by the Czochralski technique.

Because of the difficulty in growing adequate size KLN single crystals for millimeter wave characterization, we have produced cold-pressed sintered ceramics for this purpose. Figure 6 shows the dielectric constant as a function of temperature for ceramic KLN which was fired at 1045°C. This material has a very high Curie temperature of 534°C and a relatively low room temperature dielectric constant of 91, characteristics which are typical of large unit cell bronzes. The low frequency (100 Hz - 100 kHz) losses are low, being 0.007 - 0.008 over this frequency range. BSKNN ceramic material has also been prepared for direct comparison with KLN samples at millimeter wave frequencies, and typical low frequency dielectric data for the ceramic composition $Ba_{1.2}Sr_{0.8}K_{0.75}Na_{0.25}Nb_5O_{15}$ is also shown in Fig. 6. Although ceramic BSKNN has a much lower Curie point (234°C), the room temperature dielectric value is seen to be comparable to that for ceramic KLN. The millimeter wave properties of these ceramics are discussed in the next section.

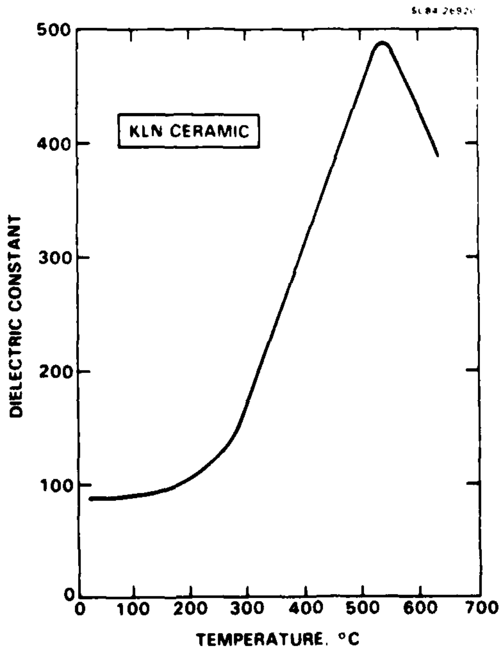

Fig. 6 10 kHz dielctric behavior of cleramic KLN.

3.4 Transmission Electron Microscopy of SBN Crystals

Single crystals of SBN commonly contain striations which can be observed in the (001) plane using polarized light microscopy. It is only recently that striation-free, high quality SBN:60 single crystals have been grown by the Czochralski techniuqe using automatic diameter control to minimize temperature gradients. Still, the presence of striations remains as a problem for other SBN compositions, as well as for other bronzes such as BSKNN. In order to determine if these optical defects are associated with physical phenomena such as stacking faults, twins or dislocations which might give rise to poor millimeter wave dielectric behavior, transmissions electron microscopy (TEM) was initiated on several SBN:60 crystals with a relatively high density of striations.

For the TEM examinations, thin sections were cut parallel to the c-axis, and were thinned to about 50 μm using wet-lapped silicon carbide papers and then mounted on a copper support grid. Before the final thinning of the specimens, they were examined using a polarized light microscope to confirm that striations were still present in the area of crystal to be studied. The sections were then thinned to electron transparency by argon ion milling and coated with carbon to prevent charging.

The thinned specimens were carefully examined at several different magnifications. At low magnification there was some evidence of preferential thinning of the crystals but the thinning showed no correlation with the striation pattern observed by optical microscopy. Tilting of areas of the specimen through several different diffracting conditions was used to scan for crystallographic features, such as faults and disloations, that might be associated with striations. However, no such crystallographic defects were observed. The only significant features which could be observed in the crytals were a high density of microstriations which ran parallel to the [001] direction, as is shown in Fig. 7. Since the striations observed by optical microscopy are much more coarse and are orthogonal to the microstriations observed by TEM, it is unlikely that the two forms of striae are associated with each other. Furthermore, the microstriations were observed to fluctuate under the TEM beam and

SC83-23775

Fig. 7 Micro-ferroelectric domains in an SBN:60 single crystal observed by TEM.

would disappear altogether as the crystal heated up to the Curie temperature. This fact suggests that the observed contrast is due to ferroelectric micro-domain walls.

At present we are attempting to develop techniques which will permit us to examine thin sections of poled SBN crystals using TEM. The major problem associated with this is the relatively low Curie temperature for SBN:60 (72°C), making partial or complete depolarization of the material likely with normal thinning procedures. Depolarization problems associated with TEM beam heating of the specimen can be alleviated with lower beam currents, complete carbon coating of both sides of the specimen for good thermal conduction to the support structure, and careful temperature monitoring. Therefore, with modified processing procedures, we anticipate being able to observe the effects of poling and thermal depolarization on the micro-domain structure.

3.5 Millimeter Wave Measurements

The most significant finding in our recent measurements is the discovery that microwave dielectric losses in the tungsten bronze ferroelectrics are strongly temperature dependent far below their respective Curie points. The polar axis loss tangent in SBN:60, for instance, is found to decrease by an order of magnitude between room temperature and 77K for frequencies between 30 and 50 GHz. This finding gives cause for renewed interest in ferroelectric modulators and phase shifters for millimeter waves in applications where cooling is possible.

From the viewpoint of modeling the dielectric properties, this unexpected dependence provides a new way to probe for the underlying mechanisms. We have begun a systematic exploration of low-temperature properties which shows that both the frequency and the orientation dependence of permittivity and loss are substanially affected. To date, results have been obtained by waveguide transmission and reflection measurements on two tungsten bronzes in single crystal and ceramic form. Preliminary observations on gadolinium molybdate and PLZT have also been made, but the work is not sufficiently complete to be reported at this time.

Our results on SBN:60 and BSKNN are summarized in Table 3 and the accompanying figures. At liquid nitrogen temperature, one finds that the polar axis permittivity has decreased by a factor of two to four, while the loss tangent along this axis has dropped by one or two orders of magnitude. Perpendicular to the polar axis in SBN, both permittivity and loss (ε'') decrease by about 30%. In BSKNN ceramic, whose dielectric properties are a mixture dominated by the two orientations perpendicular to the polar axis, ε'' drops about 40%, but remains about an order of magnitude larger than the polar axis ε''.

Figure 8 shows the effect of cooling on the frequency dependence of the polar axis loss in SBN:60 over the range 32 to 50 GHz. At room temperature (upper curve) one observes a roughly linear decrease from $\varepsilon'' = 127$ at 34 GHz to $\varepsilon'' = 50$ at 50 GHz, while at 77K (lower curve) one finds $\varepsilon'' = 5$, independent of frequency. For the same sample, the polar axis permittivity shows little

Table 3

Measured Millimeter Wave Dielectric Properties of Various Single Crystal and Ceramic Bronzes

	ϵ'	ϵ''	tan δ
SBN (60/40) c-axis (30 - 50 GHz)			
Room temperature	120 - 250	50 - 150	0.3 - 1.0
LN_2	50 - 70	2 - 8	0.04 - 0.10
SBN (60/40) a-axis (45 GHz)			
Room temperature	166	49	0.30
LN_2	116	33	0.28
BSKNN c-axis (30 - 50 GHz)			
Room temperature	60	8.4	0.15
LN_2	29	1.1	0.04
BSKNN Ceramic (45 GHz)			
Room temperature	275	64	0.23
LN_2	236	37	0.16

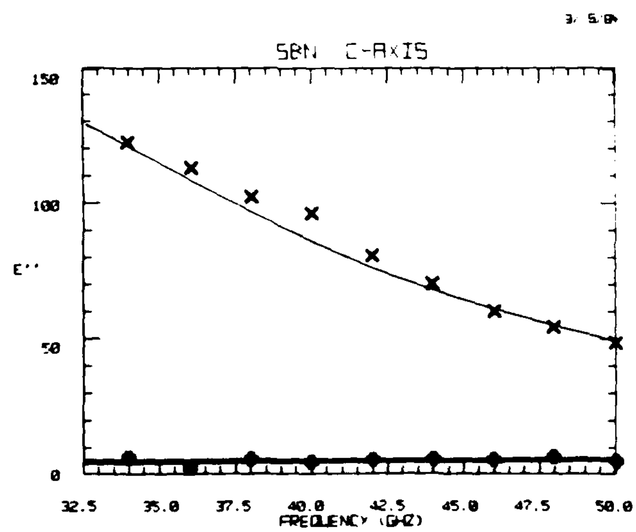

Fig. 8 Millimeter wave dielectric loss for c-axis SBN:60. Upper curve - room temperature; lower curve - 77K.

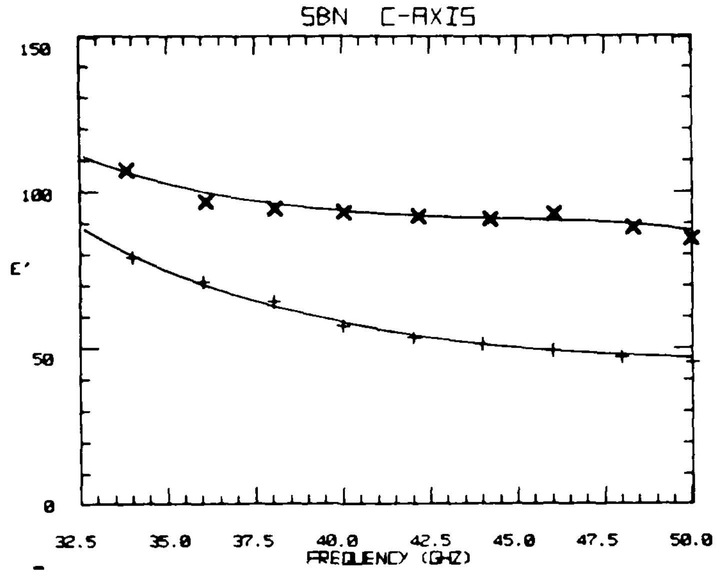

Fig. 9 Millimeter wave permittivity for c-axis SBN:60.
Upper curve - room temperature; lower curve - 77K.

dispersion at room temperature (Fig. 9, upper curve) with ε" = 100 over the whole frequency span. The low temperature behavior of the permittivity, shown in the bottom curve of Fig. 9, displays a 50% decrease from 30 to 50 GHz, with most of the drop occurring at the low frequncy end of this range. The form of this dispersion is suggestive of a loss peak centered well below 30 GHz.

To better characterize the transition to low loss in SBN:60, a second sample was heated in stages from 196°C (77K) to +50°C, and the polar axis permittivity and loss were determined at several intermediate temperatures. The most striking feature of these observations, as shown in Fig. 10, is the appearance of a peak in ε" around -50°C. This suggests a relaxation process whose characteristic rate is temperature sensitive, and coincides with the measurement frequency (44 GHz) at -50°C. A similar peak has been found in SBN samples from other growths. A repetition of these measurements at substantially higher and lower frequencies will be required to determine whether this rate is increasing or decreasing with temperature.

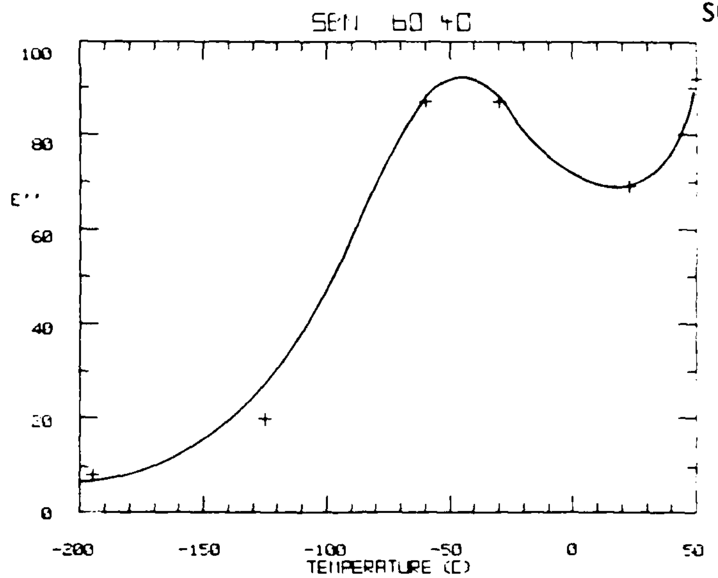

Fig. 10 Millimeter wave dielectric loss as a function of temperature for polar (c-axis) SBN:60 at 44 GHz.

Figure 11 shows the temperature dependence of the polar axis permittivity for the same SBN sample, a monotonic increase that includes a slight shoulder near -50°C. Comparison with the 44 GHz data points in Fig. 9 reveals an interesting fact: although the room temperature values of ε" differ by a factor of two between these samples, the liquid nitrogen permittivities are essentially equal. This behavior, if it is borne out in other samples from different growths, strongly suggests that the polar axis permittivity is the sum of an "extrinsic" susceptibility that dies out at low temperature, and a smaller "intrinsic" susceptibility that is not sensitive to conditions of crystal growth.

We have also measured the temperature variations of the complex polar axis permittivity in samples of barium strontium potassium sodium niobate (BSKNN). Figure 12 summarizes the results for both ε' and ε". The pattern of increasing susceptibility with increasing temperature found in SBN is also evident here, but the peak in the loss is not seen. Possibly such a peak will be found at higher temperature, corresponding to the higher Curie point of BSKNN (234°C) as compared to 72°C for SBN:60.

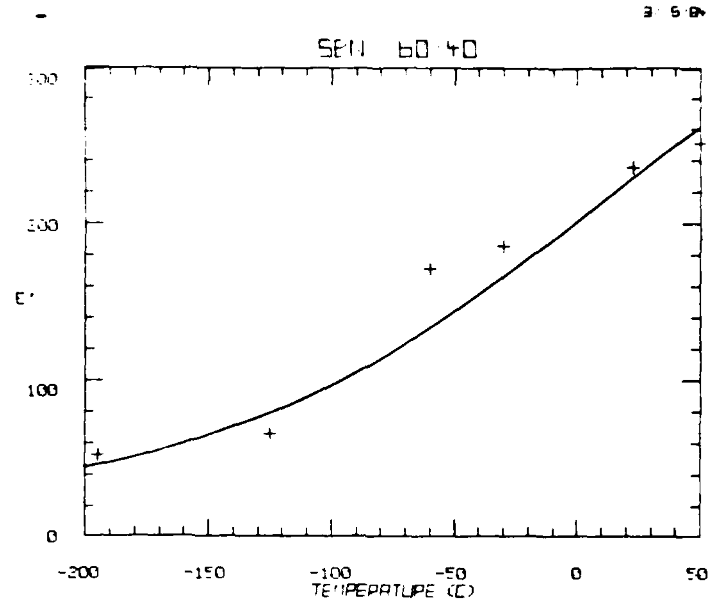

Fig. 11 Millimeter wave permittivity as a function of temperature for polar (c-axis) SBN:60 at 44 GHz.

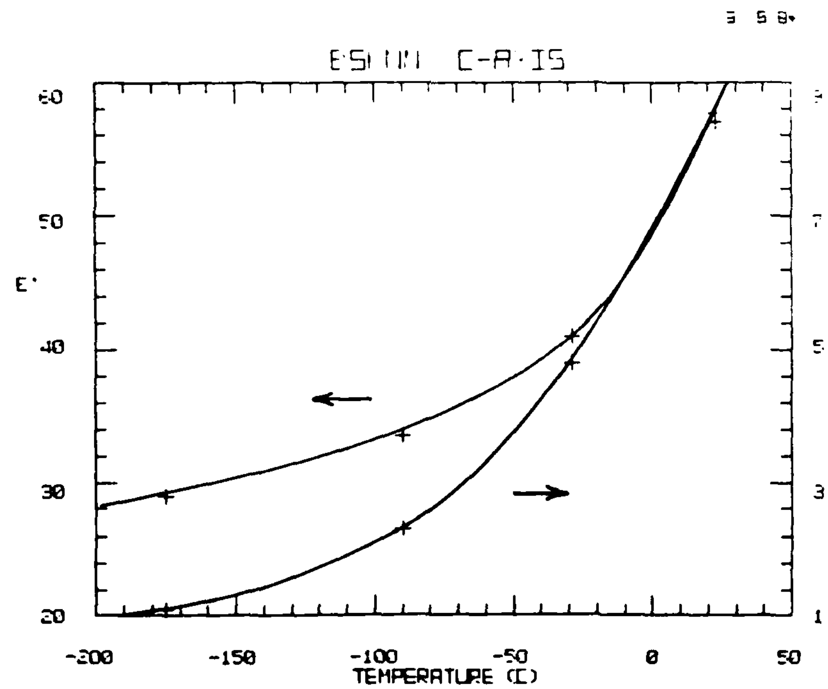

Fig. 12 Polar axis BSKNN dielectric properties as a function of temperature at 44 GHz.

Figures 13 and 14 illustrate the frequency dependence of the measured power reflection and transmission coefficients for a 0.65 millimeter thick sample of BSKNN. The reflection minima and transmission peaks occur for half-wave optical thickness; they would be unobservable if the loss tangent were near unity, as it is in SBN. It is worth noting that the transmission maximum at -175°C corresponds to less than 2 dB insertion loss, which means that devices such as modulators or phase shifters based on cooled BSKNN could compare favorably with existing ferrite technology. A general summary of the present observations on SBN and BSKNN is given in Table 4.

Table 4
Summary of Millimeter Wave Observations

- Dielectric loss drops drastically with temperature in all single crystal samples along polar axis.
- Moderate decrease in dielectric constant observed at low temperatures.
- Temperature effect minimal perpendicular to polar axis.
- Insertion loss less than 3 dB for samples with millimeter thicknesses.
- Qualitative behavior suggests loss mechanism due to acoustical phonons.

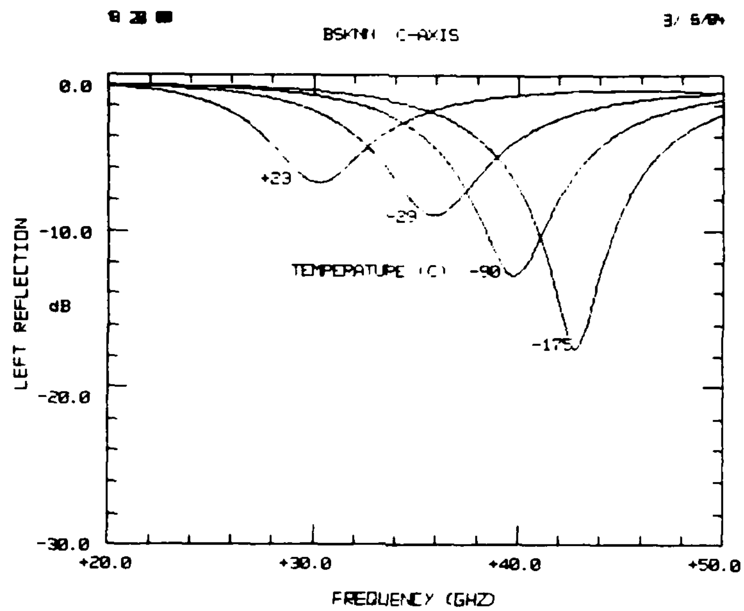

Fig. 13 Polar axis BSKNN millimeter wave reflection as a function of frequency and temperature (t = 0.65 mm).

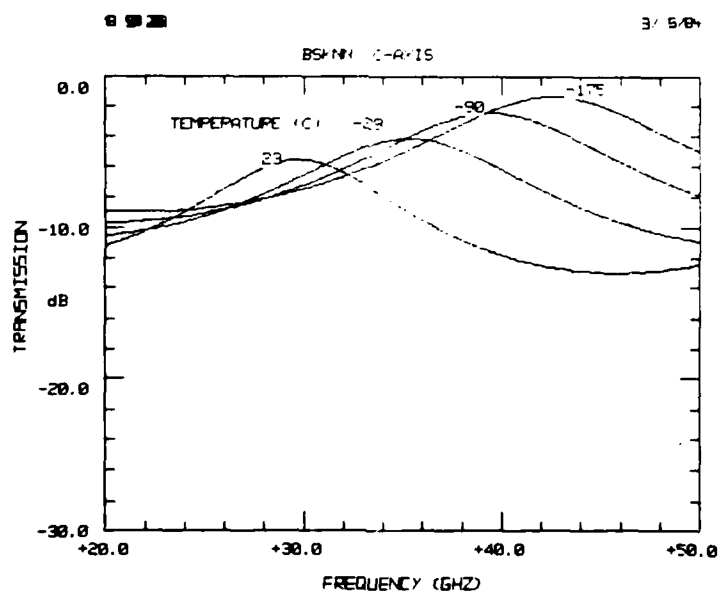

Fig. 14 Polar axis BSKNN millimeter wave transmission as a function of frequency and temperature (t = 0.65 mm).

4.0 PROPOSED WORK

4.1 Role of Dopants in SBN Crystals

Since the general quality of SBN crystals has now been substantially improved, it is of interest to investigate the role of dopants in this bronze material as they affect the millimeter wave dielectric properties, particularly at room temperature. As discussed earlier, both Ce^{3+} and Fe^{3+} dopants have been successfully incorporated in SBN:60 single crystals grown by the Czochralski technique, albeit with some growth difficulties (e.g., cracking) and a moderate degradation in crystal quality from an optical standpoint. In future research we plan to expand this work in order to grow larger and better quality doped SBN:60 crystals under DARPA contract and to determine to what extent, if any, the presence of dopant ions modifies the dielectric permittivity and losses at millimeter wave frequencies.

There is a definite parallel between the material requirements for millimeter wave devices and those for photorefractive and electro-optic applications. At optical frequencies the change in the refractive index is given by

$$\Delta n_i = \frac{1}{2} n_i^3 r_{ij} E_j$$

where r is the electro-optic coefficient and E is the electric field. For photorefrative applications it is desirable to improve both the space charge field E and the electro-optic r coefficients which are linearly related to the value of the polarization P_s and the low frequency ε_{ij}. Initial measurements on Fe^{3+}- and Ce^{3+}-doped SBN:60 crystals have shown a substantial increase in the room temperature value for ε_{33} with only minor changes in ε_{11} and ε_{22} over undoped material. Photorefractive measurements on Ce-doped SBN:60 crystals have shown a photorefractive sensitivity of 9.5×10^{-3} cm^2/J, a value that exceeds that of Fe-doped $LiNbO_3$ by more than two orders of magnitude. These results are significant and point to areas of future investigation.

Based on our crystal chemistry work on tungsten bronze SBN:60 and SBN:50 single crystals and ceramics, the incorporation of 3-d or 4-f ions in the lattice should be advantageous for both millimeter wave and optical device applications. Table 5 shows several proposed dopant ions for this work and their lattice site preferences. Since the effect of these ions on millimeter wave dielectric losses is not yet well established, it may prove worthwhile to examine non 3-d and 4-f ions such as Ca^{2+}, W^{6+}, etc. as dopants in order to gain a better understanding of the millimeter wave dielectric losses and possible mechanisms. A thorough understanding of dopant valence states, site preferences and the effects of dopant concentration is fundamental to this work and will be explored in depth.

Table 5
Proposed Dopants for Millimeter Wave Studies in SBN

		Site Preference for the Proposed Dopants			
Dopants	Valence State	15-Fold	12-Fold	9-Fold	6-Fold
Cerium	Ce^{3+}, Ce^{4+}	Ce^{3+}	Ce^{3+}	Ce^{4+}	Ce^{4+}
Terbium	Tb^{3+}, Tb^{4+}	--	Tb^{3+}	Tb^{4+}	Tb^{4+}
Iron	Fe^{3+}, Fe^{2+}	--	--	Fe^{2+}	Fe^{2+}, Fe^{3+}
Manganese	Mn^{2+}, Mn^{3+}, Mn^{4+}	--	--	Mn^{2+}	Mn^{2+}, Mn^{3+}
Titanium	Ti^{4+}, Ti^{3+}	--	--	--	Ti^{4+}, Ti^{3+}
Molybdenum	Mo^{6+}, Mo^{4+}	--	--	--	Mo^{6+}, Mo^{4+}
Niobium	Nb^{5+}, Nb^{4+}	--	--	--	Nb^{5+}, Nb^{4+}

4.2 SBN Single Crystal Development

To date, work has focussed on the composition $Sr_{0.60}Ba_{0.40}Nb_2O_6$ in the SBN system, since it is this composition which has been the most extensively developed in single crystal form. Other compositions, however - specifically SBN:75 and SBN:50 - are also of interest and may provide further insight into the millimeter wave behavior of the dielectric properties as a function of composition. Unlike SBN:60, these two compositions are not congruent melting, and hence they are difficult to grow by the Czochralski technique, with the main problem being one of bulk fracture during growth. Nevertheless, boules as large as 1.0 cm in diameter have been grown with some crack-free regions.

Based on the experience gained with the implementation of automatic diameter control in the growth of SBN:60, the growth work on SBN:50 and SBN:75 will be resumed with an eye toward producing larger and better quality single crystals. SBN:75 is particularly interesting for millimeter wave and photorefractive device applications because of its high room temperature dielectric constant at low frequencies and its high electro-optic coefficient. A summary of the dielectric and optical properties of these bronzes, and others, is given in Table 6. It will be interesting to observe what changes in the millimeter wave dielectric properties occur with changes in SBN composition in order to further the understanding of the response of bronze materials at these frequencies, particularly with regard to the mechanisms behind the dielectric losses as a function of temperature.

Table 6
Physical Properties of Various Ferroelectric Crystals

Property	SBN:75	SBN:60	SBN:50	$LiNbO_3$	$LiTaO_3$
Point Group	4 mm	4 mm	4 mm	R3C	R3C
Dielectric Constant*	ε_{33} = 3400	ε_{33} = 500	ε_{33} = 450	ε_{33} = 60	ε_{33} = 58
Electro-optic 10^{-12} m/V	r_{33} = 1350 r_{13} = 70 r_{51} = 42	r_{33} = 420 r_{13} = 55** r_{51} = 80	r_{33} = 180 r_{13} = 35 r_{51} =	r_{33} = 31 r_{13} = 9.5 r_{51} = 23	r_{33} = 30 r_{13} = 7.5 r_{51} = 20
Curie Temperature Tc (°C)	56	72	120	1150	660

* After poling
** Interpolated

4.3 Millimeter Wave dn/dE Measurements

The dramatic decrease in millimeter wave dielectric losses at low temperatures now makes it imperitive to examine the value of dn/dE from liquid nitrogen up to and beyond room temperature. To date such measurements have been limited to a small range near room temperature because of contact loss and/or sample shifting in the waveguide. The present arrangement with a free-standing dielectric specimen contacted by rigid contact probes at the top and bottom is inadequate for reliable measurements over a wide temperature range because of the problems created by waveguide and sample expansion/contraction. We are presently considering the use of a slightly recessed waveguide flange which can hold the specimen firmly in place and permit more reliable contacts, including possibly wire-bonded, to be used. We anticipate that this work will be completed well before the end of the next reporting period.

5.0 SUMMARY OF TASKS

- The composition $Pb_{0.6}Ba_{0.4}Nb_2O_6$, which is close to the morphotropic phase boundary in the $Pb_{1-x}Ba_xNb_2O_6$ system, will be hot pressed to study its high frequency dielectric properties.

- Initiate high frequency dielectric measurement on fully stuffed tungsten bronze $K_3Li_2Nb_5O_{15}$ ceramic and single crystal samples. This material should exhibit low losses at high frequency.

- Carry out structure factor analysis to identify the site preference for various cations, specifically on the 15- and 12-fold coordinated sites, and their role in improving the high frequency dielectric losses.

- Low-temperature loss peak: The maximum in polar axis dielectric loss found near -50°C in SBN:60 will be further explored to determine its freeqUency dependence and variation with growth conditions. Measurements on BSKNN will be pushed to higher temperatures to look for a similar loss peak in that material.

- The apparent convergence in millimeter wave permittivity values found for different growth conditions of SBN:60 at liquid nitrogen temperatures will be investigated for a wider range of SBN samples.

- The temperature dependence of millimeter wave dielectric properties perpendicular to the polar axis will be studied at temperatures well below 77K, to determine whether the high losses in SBN and BSKNN in this orientation will also freeze out.

6.0 REFERENCES

1. H. Fetterman, C. Hu, W.E. Bauch and C.D. Parker, MIT Solid State Research Report 2, 30 (1975).

2. K. Megumi, N. Nagatsuma, Y. Kashiwada and Y. Furuhata, J. Mat. Sci. 11, 1583 (1976).

3. R.R. Neurgaonkar and L.E. Cross, DARPA Final Report, Contract No. F49620-78-C-0093 (1982).

4. C.E. Land and P.D. Thacher, Proc. IEEE 57, 751 (1969).

5. G.H. Haertling and C.E. Land, J. Am. Ceramic Soc. 54, 1 (1971).

6. G.H. Haertling, J. Am. Ceramic Soc. 54, 303 (1971).

7. M. Yokosuka, Jap. J. Appl. Phys. 16, 379 (1977).

8. K. Nagata and K. Okazaki, Japan-U.S. Study Seminar on Dielectric and Piezoelectric Ceramics, No. W-11 (1982).

9. J.R. Oliver (unpublished data).

10. R.R. Neurgaonkar, AFOSR Final Report, Contract No. F49620-81-C-0005 (1982).

APPENDIX 1

DIELECTRIC PROPERTIES OF FERROELECTRIC TUNSTEN BRONZE $Ba_{2-x}Sr_xK_{1-y}Na_yNb_5O_{15}$ CRYSTALS AT RF AND MILLIMETER WAVE FREQUNCIES

W.W. Ho, W.F. Hall and R.R. Neurgaonkar

Ferroelectrics, Vol. 50, pp 325-330, 1983

Rockwell International
Science Center

DIELECTRIC PROPERTIES OF FERROELECTRIC TUNGSTEN BRONZE $Ba_{2-x}Sr_xK_{1-y}Na_yNb_5O_{15}$ CRYSTALS AT RF AND MILLIMETER WAVE FREQUENCIES

W.W. HO, W.F. HALL, AND R.R. NEURGAONKAR
Rockwell International Science Center, Thousand Oaks, CA 91360

Abstract Permittivity and dielectric loss have been measured for a number of single crystal samples of barium strontium potassium sodium niobate (BSKNN) in three frequency ranges: 0-1 MHz, 30-40 GHz, and 90-100 GHz. This work is part of an ongoing study of millimeter wave properties of ferroelectrics with potential applications in active components such as phase shifters, modulators, and switches. BSKNN has been selected as typifying one extreme in the tungsten bronze family, where all 15- and 12-fold coordinated cation sites are occupied. Measurements on these crystals show significantly lower millimeter wave absorption than is found in strontium barium niobate (SBN) crystals grown by the same techniques. The permittivities along the principal crystal axes showed a substantial decrease with increasing frequencies over the range of observations, which may be indicative of a relaxation mechanism occurring in the GHz frequency region.

INTRODUCTION

The millimeter wave dielectric properties of ferroelectric materials are largely unexplored. From an experimental viewpoint, measurements were difficult due to typically high dielectric constants, while from a theoretical viewpoint, it was expected that the low frequency properties could be reliably extrapolated to a few hundred gigahertz, so long as the material was not too close to its Curie temperature. However, the need for means to modulate microwave energy at millimeter wavelengths has led us to initiate a detailed study of the linear and nonlinear susceptibilities of the available ferroelectrics, and the results, in the main, do not fit within the accepted picture.

We have taken as a model system the tungsten bronze ferroelectrics, which are known to exhibit very large dielectric susceptibilities at both low frequency and optical wavelengths. Growth of these compounds in a single crystal form is itself a major undertaking, which has been pursued at our laboratory as part of a long-range effort to develop ferroelectric materials. Single crystal materials examined to date include strontium barium niobate (SBN)[1], strontium potassium niobate (SKN)[2], and barium strontium potassium sodium niobate (BSKNN). In addition, ceramic samples of various perovskite and tungsten bronze ferroelectrics have been studied.

The common feature found in all these systems at millimeter wave frequencies is a marked decrease in permittivity from its low-frequency value, accompanied by a large increase in dielectric loss. Because the measurement frequencies are so far below any intrinsic crystal resonances, including soft phonon modes, it appears that this dispersion must be due to defects or disorder in the crystal structure. In part to test this contention, BSKNN was chosen as typifying the most ordered structure among the tungsten bronzes. In this crystal, all 15- and 12-fold coordinated cation sites are occupied.

MEASUREMENTS ON BSKNN

The experimental procedure used in our laboratory for determining dielectric properties of high-index materials has been described elsewhere[1]. In the present instance, several single crystal samples of BSKNN cut to fill the waveguide cross-section were studied from 30-40 GHz and from 90-100 GHz. Power reflection and transmission coefficients were measured in each band of frequencies and complex permittivities $\varepsilon' + i\varepsilon''$ were determined by fitting to these measured values. Tables I-IV summarize the results of this procedure at selected frequencies in each band for the two polarizations of the microwave electric field, namely parallel and

BSKNN: MILLIMETER WAVE PROPERTIES

TABLE I BSKNN — c-axis.

f, GHz	ε'	ε"
30	360	10.9
33	300	16.4
36	265	23.9
39	240	24.9

TABLE II BSKNN — a-axis.

	Sample #a		Sample #b	
f, GHz	ε'	ε"	ε'	ε"
33	275	49.3	260	59.7
36	290	23.5	285	25.5
39	245	51.4	285	22.6

TABLE III BSKNN — c-axis.

	Sample #1		Sample #2		Sample #3		Sample #4	
f, GHz	ε'	ε"	ε'	ε"	ε'	ε"	ε'	ε"
92	57	10.4	56	9.95	52.5	11.5	50	12.7
94	54	11.3	54	10.8	50	11.2	50	12.8
96	52	11.2	52	10.9	50	10.5	57.5	13.7
98	50	11.3	50	10.9	55	10.1	55	13.1

TABLE IV BSKNN — a-axis.

	Sample #1		Sample #3		Sample #4	
f, GHz	ε'	ε"	ε'	ε"	ε'	ε"
92	47.5	27.4	95	26.7	93	28.7
94	55	34.2	95	30.0	108	34.8
96	60	35.9	100	29.2	100	36.7
98	70	34.0	100	26.1	100	35.9

perpendicular to the crystal polar (c-) axis.

In Table II, results are given for the perpendicular permittivity on two samples cut from the same boule. The sample-to-sample variability shown here is fairly typical. In the higher frequency band, four samples were measured for each polarization (results for a-axis sample #2 are omitted from Table IV for reasons discussed below). All samples show substantial decrease in their real permittivity from the values at 30 GHz, accompanied by increases in the loss tangent $\tan\delta = \varepsilon''/\varepsilon'$, primarily due to the decrease in ε'.

The fit for a-axis sample #2 between 90 and 100 GHz did not produce a unique value for the permittivity, due to an unfortunate convergence of roots in the expressions for the reflected and transmitted power. Values of ε' ranging from 200 to 500 gave equally valid fits. Values for ε'' were more grouped, and showed a definite increasing trend within the band, ranging from about 30 ±3 at 92 GHz to 40 ±5 at 98 GHz.

Preliminary low-frequency measurements on poled BSKNN samples showed room-temperature permittivities varying in the range 230 to 430 along the polar axis. We are currently investigating factors such as incomplete poling which could give rise to this scatter in measured properties. Peak permittivities near the Curie point varied from 15,000 to 25,000. Perpendicular to the polar axis, the permittivity was typically frequency independent up to 1 MHz at values near 400 and exhibited a slight (15%) increase near T_c.

Compared with our earlier measurements on SBN[1], the high-frequency dielectric loss along the polar axis in these BSKNN samples is much smaller. In the band between 30 and 40 GHz, typical values for ε''_{33} in SBN are 40 to 60, with $\tan\delta_{33}$ near 0.2; in BSKNN, we find ε''_{33} to lie between 10 and 25, and $\tan\delta_{33}$ ranges from 0.03 to 0.1. Perpendicular to the polar axis, BSKNN tends to show greater loss, comparable to similarly oriented samples of SBN.

BSKNN: MILLIMETER WAVE PROPERTIES

INTERPRETATION

The most striking feature of the millimeter wave measurements on tungsten bronze ferroelectrics to date is the high loss and dispersion in dielectric properties compared with the low frequency behavior of these same materials. The Devonshire model which fits this low frequency behavior is generally understood to reflect the dominance of a single soft mode in the dielectric response; this mode residing above 1000 GHz at room temperature and moving into the measurement range as the Curie point is approached.

There is no room in such a model for a rapid dispersion in the GHz range at room temperature. The observed behavior is suggestive of piezoelectric resonance, spread over a broad frequency range by a corresponding spread in the characteristic dimension of the resonating regions. Such regions might be microdomains stabilized by localized defects. However, one would then expect sensitivity of the high-frequency loss to the details of the poling procedure, and this is not observed. Losses in poled and unpoled samples of SBN were found to be indistinguishable.

Another possibility, which we are only now in the process of exploring, is that growth defects can themselves provide a strong, non-resonant piezoelectric coupling to heavily damped elastic waves. It has long been known that high-frequency acoustic waves in soft-mode ferroelectrics are strongly attenuated[3]. If dislocations in the ferroelectric produce large local gradients in the polarization, the microwave electric field can drive these dislocations to produce acoustic radiation. In the most favorable case, the rate of dissipation by this process can approach half the maximum resonant loss in the same volume of material.

REFERENCES

1. W.W. Ho, W.F. Hall, R.R. Neurgaonkar, R.E. DeWames, and T.C. Lim, Ferroelectrics 38, 833 (1981).

2. R.R. Neurgaonkar, W.K. Cory, W.W. Ho, and W.F. Hall, Ferroelectrics 38, 857 (1981).
3. H.H. Barrett, in W.P. Mason and R.N. Thurston, Physical Acoustics, Vol. VI, p. 65, Academic Press (New York, 1970).

APPENDIX 2

LOW AND HIGH FREQUENCY DIELECTRIC PROPERTIES OF FERROELECTRIC TUNGSTEN BRONZE $Sr_2KNb_5O_{15}$ CRYSTALS

R.R. Neurgaonkar, W.W. Ho, W.K. Cory, W.F. Hall and L.E. Cross

Accepted for Publication in Ferroelectric (1984)

Rockwell International
Science Center

LOW AND HIGH FREQUENCY DIELECTRIC PROPERTIES OF FERROELECTRIC TUNGSTEN BRONZE $Sr_2KNb_5O_{15}$ CRYSTALS

R.R. Neugaonkar, W.W. Ho, W. K. Cory & W. F. Hall
Rockwell International
Microelectronics Research & Development Center
1049 Camino Dos Rios
Thousand Oaks, California 91360

&

L. E. Cross
Materials Research Laboratory
Pennsylvania State University
University Park, PA. 16802

ABSTRACT

Single crystals of $Sr_2KNb_5O_{15}$ (SKN), approximately 5-8 mm in diameter and 10-20 mm long, have successfully been grown by the Czochralski technique. The crystal has ferroelectric tetragonal tungsten bronze structure with a curie temperature of about 150°C. The dielectric and electromechanical coupling constants for this crystal have been established: the polar axis dielectric constant, K_{33} exceeds 20,000 at the curie temperature while the coupling constants are k_{33}= 0.52 and k_{31} = 0.19, respectively. High frequency dielectric properties of SKN samples were also determined between 90-100 GHz. These measurements indicated that the bulk of the polar axis permittivity has relaxed below 90GHz, implying that the low frequency dielectric response is not soft-mode controlled.

INTRODUCTION

The high dielectric permittivities found in many classes of ferroelectrics are variously ascribed to soft lattice modes, Debye relaxation, and ionic tunneling. These classes of materials offer interesting potential for device applications, and it is therefore desirable to explore the range of properties which can be achieved and to establish the mechanisms controlling these properties. In this work, we have developed growth techniques for the single crystal tungsten bronze strontium potassium niobate ($Sr_2KNb_5O_{15}$) and have characterized the dielectric peoperties at frequencies up to 100 GHz. Electromechanical coupling constants have also been determined.

RESULTS AND DISCUSSION

System $SrNb_2O_6$-$KNbO_3$:

Ferroelectric alkali-alkaline earth niobates having tetrogonal tungsten bronze structure, e.g. $Sr_2KNb_5O_{15}$ (SKN), show considerable promise since they exhibit excellent dielectric and optical properties (1-3). The cited SKN composition exists on the pseudobinary $SrNb_2O_6$-$KNbO_3$ system and melts around 1470°C. It is also known that the Sr:K ratio can be changed while still maintaining the tetragonal tungsten bronze structure even though neither of the end members has this structure. Other examples of this behavior can be found in the $SrNb_2O_6$-$BaNb_2O_6$ and $BaNb_2O_6$-$KNbO_3$ (4-7) and related systems.

Before the single crystal growth of SKN was attempted, the phase relation in the $SrNb_2O_6$-$KNbO_3$ system was reinvestigated since there is disagreement between the results reported by Scott, et. al (6) and Ainger, et al (8) on this system. According to Scott, et al, the congruent melting composition of 77 mole% is suitable for the growth studies, while Ainger, et al, claimed that the potassium deficient composition, $K_{.5}Sr_{2.5}Nb_5O_{15}$ (84 mole% $SrNb_2O_6$) is the congruent melting composition. Although the results of this study are not complete, it has been shown that the composition close to 77 mole% (after Scott, et al) is suitable for the single crystal growth of SKN:

hence the composition represented by formula 75 mole% $SrNb_2O_6$ (75 mole% $SrNb_2O_6$ + 25 mole% $KNbO_3$) has been selected in the present work.

Bulk Single Crystal Growth Procedure

Single crystals of SKN were successfully grown by the Czochralski technique from both platinum and iridium crucibles. In the case of the iridium crucibles, argon pressure had to be used to prevent excessive loss of iridium, and as-grown crystals were found to be purple to coal black in color. However, the color changed to deep yellow when the crystals were annealed in oxygen over 1000°C. Oxygen pressure was directly employed when crystals were pulled from platinum crucibles; crystals thus obtained are pale yellow in color. Since lattice mismatch between SKN and $Sr_{.6}Ba_{.4}Nb_2O_6$ (SBN) bronze composition is minimal, SBN single crystals were used as seed material in the present crystal growth work. This proved to be very successful and SKN single crystals as large as 5-8 mm in diameter and 10-20 mm long have been grown. Optimum conditions used are as follows:

Pulling Rate:	5-8 mm/hr
Rotation Rate:	15-25 rpm
Growth Direction:	Along the c-axis
Growth Temperation:	1475°C

The crystals were also pulled along other directions, e.g. (100) and (110), and under different experimental conditions. However, it was found difficult to grow crystals along these directions. This clearly suggested that the rate of crystallization along the c-axis is much faster than those along any other directions. Fig. 1 shows a typical 5-8 mm in diameter and 20 mm long SKN crystal grown along the c-axis. The growth of SKN single crystals have also been reported by Giess et al (1) and Ainger, et al (8); however, the size and quality of crystals obtained is not clear from their work. Based on our ongoing research work on other tungsten bronze crystals having compositions, $Sr_{1-x}Ba_xNb_2O_6$, x = 0.6 and 0.5, (9,10) and $K_3Li_2Nb_5O_{15}$ (11), there is a great deal of similarity among these crystals and it has been found that the growth of these crystals depends strongly on the ability to control the diameter of crystal and the thermal gradient in the crystal near the solid-liquid interface. This is a difficult task, but it has been successfully accomplished for the present crystals.

LOW FREQUENCY DIELECTRIC CHARACTERISTICS

Optically the SKN single crystals appear to be of excellent quality, and they are clear and transparent. Crystals grown along the c-axis are usually faceted, which is quite exceptional for the Czochralski grown crystals. X-ray diffraction studies show that the crystal habits are based on 24 facets of four prism:(110), (120), (100), and (130). In present case, the SKN crystals showed several of such facets, but all of them are not as well-defined as reported for the tungsten bronze $Sr_{1-x}Ba_xNb_2O_6$, x= 0.6 and 0.5 solid solution single crystals (9, 10). The results of this study indicate that the appearance of these facets depends strongly on the growth conditions and they change markedly or disappear by varying the growth temperature. The lattice constants measurement for the ceramic and single crystal samples of 75 mole% (75% $SrNb_2O_6$ + 25% $KNbO_3$) composition gave the values of a = 12.458 Å and c= 3.944 Å, which are in close agreement with the values a= 12.470 Å and c= 3.942 Å reported by Giess, et al (7) for 77 mole% composition. The density of the single crystal is 4.976 gm/cm^3, which corresponds to two molecules of $Sr_2KNb_5O_{15}$ per unit cell.

Low frequency dielectric measurements were initiated on the SKN single crystals and the results obtained are very interesting. The temperature dependences of the capacitance were measured over the temperature range -50° to 200°C at three different frequencies, i.e. i, 10, 100 KHz. As shown in Fig. 2, at room temperature the dielectric constant K_{33} is 2 x 10^2 and peaks above 10^4 at the curie temperature. The dielectric constant at the curie temperature on our current crystal exceeds over 20,000, which is substantially higher than the dielectric constant reported by Giess, et al (1) for their SKN single crystal. Above the transition temperature a curie weiss law $K_{33} = C/(T-T_c)$, is found to hold for the crystals measured with C in the range 2-4 x 10^2 °C. Fig. 3 shows the temperature dependence of the dielectric loss for SKN crystal at three frequencies: 1, 10, 100 KHz.

The electromechanical coupling constants for SKN single crystals were also established by the resonance-antiresonance technique. Prior to measurements, the crystals were poled by the field-cooling method under a dc-field of approximately 6 KV/cm along the c-axis. The coupling constants k_{33} and k_{31} were determined as 0.52 and 0.19, respectively. Table 1 summarizes the ferroelectric properties for various tungsten bronze crystals. It is clear from this data that the coupling constants for the SKN crystal are slightly higher than for the $Sr_{.6}Ba_{.4}Nb_2O_6$ crystal and are similar to those for another important bronze composition, $K_3Li_2Nb_5O_{15}$. In general, the SKN single crystal possesses excellent dielectric, electromechanical coupling constants and other physical properties and should prove to be an interesting candidate for several device applications.

HIGH FREQUENCY CHARACTERIZATION

Room-temperature reflection and transmission measurements have been carried out between 90 and 100 GHz on four small single-crystal samples cut from a single boule of SKN and oriented to allow determination of the complex dielectric permittivities parallel and perpendicular to the crystal polar axis. These measurements were made in waveguide with the sample filling the guide cross-section.

The dielectric permittivities derived from these data show a large dispersion, with K'_{33} having fallen to one quarter of its low-frequency value, while k'_{11} in this range of frequencies is about twice k'_{33}. The frequency dependence of these parameters is summarized in Figure 9. along with the dielectric loss k''_{11} and k''_{33} (upper and lower sections of the figure, respectively).

The large decrease observed in K'_{33} from its low-frequency value strongly suggests that the bulk of the polar axis permittivity is not contributed by the soft mode, which is thought to lie above 10^{12} Hz in this temperature range. Rather, mechanisms must be sought having characteristic relaxation at GHz frequencies, such as piezoelectric resonance in microdomains of submicron dimension. Point defects, or perhaps dislocations induced by compositional gradients in the crystal, may act to stabilize such domains against poling. The relatively high observed loss ($\tan \delta_{33} \sim 0.25$, $\tan \delta_{11} \sim 0.13$) and the variation in permittivity between samples from the same boule are also consistent with an extrinsic GHz relaxation mechanism.

Recently we have observed similar behavior in strontium barium niobate single crystals between 30 and 40 GHz, measured as part of an ongoing DARPA program to develop millimeter wave phase shifting materials. In one such sample, the polar axis permittivity was approximately 35 over the whole frequency range from 30 to 40 GHz, compared to a low-frequency permittivity of 900. This suggests that the phenomenon we are observing may be generally responsible for the high dc permittivities in the tungsten bronze family.

ACKNOWLEDGEMENT

This research work was supported by the ONR and DARPA Agencies under Contract No. N00014-81-C-0463 and F49620-78-C-0093.

REFERENCES

1. E.A. Giess, G. Burns, D.F. O'Kane and A.W. Smith, "Ferroelectric and Optical Properties of $Sr_2KNb_5O_{15}$" Appl. Phys. Lett. 11, 233, (1967).

2. R. Clarke and F. W. Ainger, "The Electro-optic Properties of Ferroelectric $Sr_2KNb_5O_{15}$ Crystals", Ferroelectrics, 7, 101, (1974).

3. G. Burns, E. A. Giess, D. F. O'Kane, B. A. Scott and S. W. Smith, "Properties of Tungsten Bronze Ferroelectrics", J. Phys. Soc. Jap., 28, 153, (1970).

4. M. H. Francombe, "The Relation Between Structure and Ferroelectricity in Lead Barium and Barium Strontium Niobates", Acta. Cryst., 13, 131, (1960).

5. A. A. Ballman and H. Brown, "The Growth and Properties of Strontium Barium Niobate, $Sr_{1-x}Ba_xNb_2O_6$, A Tungsten Bronze Ferroelectric", J. Cryst. Growth 1, 311, (1967).

6. B. A. Scott, E. A. Giess, D. F. O'Kane and G. Burns, "Phase Equilibria in the $KNbO_3$-$BaNb_2O_6$ and $KNbO_3$-$SrNb_2O_6$ systems," J. Am. Ceram. Soc., 53, 106, (1969).

7. E. A. Giess, B. A. Scott, G. Burns, D. F. O'Kane and A. Segmuller, "Alkali-Strontium-Barium-Lead Niobate Systems with a Tungsten Bronze Structure: Crystallographic Properties and Curie Points", J. Am. Ceram. Soc. 52, 276, (1968).

8. F. W. Ainger, J. A. Beswick, and S. G. Porter, "Ferroelectrics in the K_2O-SrO-Nb_2O_5 system", Ferroelectrics, 3, 321, (1972).

9. R. R. Neurgaonkar, M.H. Kalisher, T.C. Lim, E. J. Staples and K.L. Keester, "Czochralski Single Crystal Growth of $Sr_{.61}Ba_{.39}Nb_2O_6$ for Surface Acoustic Wave Devices", Mat. Res. Bull. 15, 1235, (1980).

10. R.R. Neurgaonkar, W. K. Cory, W. W. Ho, W. F. Hall and L. E. Cross, "Tungsten Bronze Family Crystals for Acoustical and Dielectric Applications", Ferroelectrics, 38, 857, (1981).

11. R. R. Neurgaonkar, W. K. Cory and L. E. Cross, "Single Crystal Growth $K_3Li_2Nb_5O_{15}$ and Its Ferroelectric Properties", to be published in Mat. Res. Bull.

12. T. R. Shrout, L. E. Cross, P. Moses, H. A. McKinstry and R. R. Neurgaonkar, "A Phenomenological Theory for Predicting the Temperature Dependence of Elastic Dielectric, and Piezoelectric Properties in Simple Proper Ferroelectric Crystals." Proc. of Ultrasonic Sympo., 414, (1980).

13. M. Adachi and A. Kawabata, "Elastic and Piezoelectric Properties of Potassium Lithium Niobate $K_3Li_2Nb_5O_{15}$ Crystals", Jap. J. Appl. Phys. 11, 1969, (1978).

14. T. Fukuda, "Growth and Crystallographic Characteristics of $K_3Li_2Nb_5O_{15}$ crystals", Japan J. Appl. Phys. 8, 122 (1969).

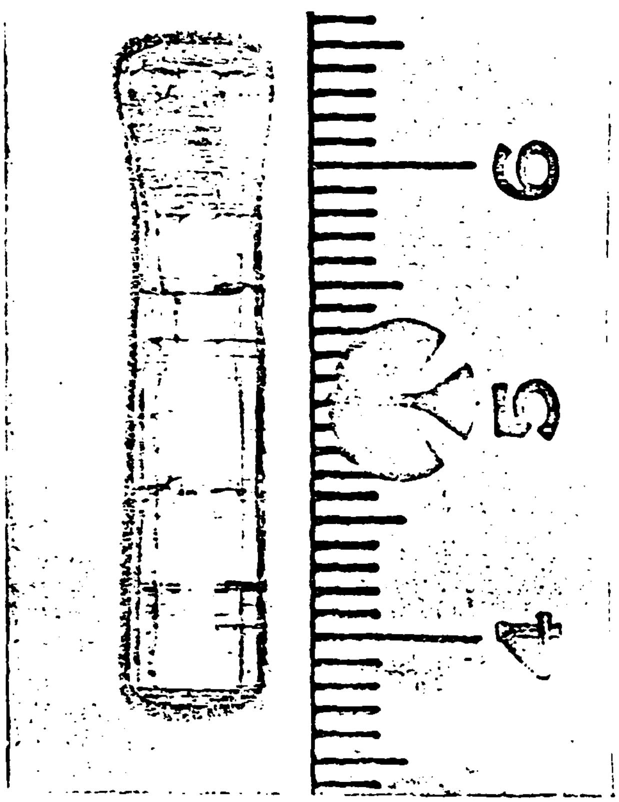

Figure 1. Shows a typical 5-8 mm in diameter $Sr_2KNb_5O_{15}$ Crystal grown along the c-axis.

PHYSICAL PROPERTIES OF VARIOUS T. B. CRYSTALS

TABLE 1

Property	SKN	SBN:60	KLN
Unit Cell	Tetragonal	Tetragonal	Tetragonal
Space Group	4mm	4mm	4mm
Unicell	a=12.47Å	a=12.468Å	a=12.59Å
Facets	Several, less defined	Well defined 24	Well defined 4
Curie Temperature °C	150° C	72° C	405° C
E_{33} at 25° C	200	880	150
E_{33} at T_c	$\geq$ 20,000	$\geq$ 40,000	~1000
Electromechanical Coupling Constant	k_{33}=0.52 k_{31}=0.19 k_{15}= -	k_{33}=0.47 k_{31}=0.14 k_{15}=0.13	k_{33}=0.54 k_{31}=0.18 k_{15} 0.35
Piezoelectric Strain Constant	d_{33}= - d_{31}= - d_{15}= -	d_{33}= 30 d_{31}=130 d_{15}= 31	d_{33}=57 d_{31}=-14 d_{15}=68
References	Present	12	13,14

SBN:60 -------$Sr_{.6}Ba_{.4}Nb_2O_6$ KLN---------$K_3Li_2Nb_5O_{15}$

FIGURE 2.

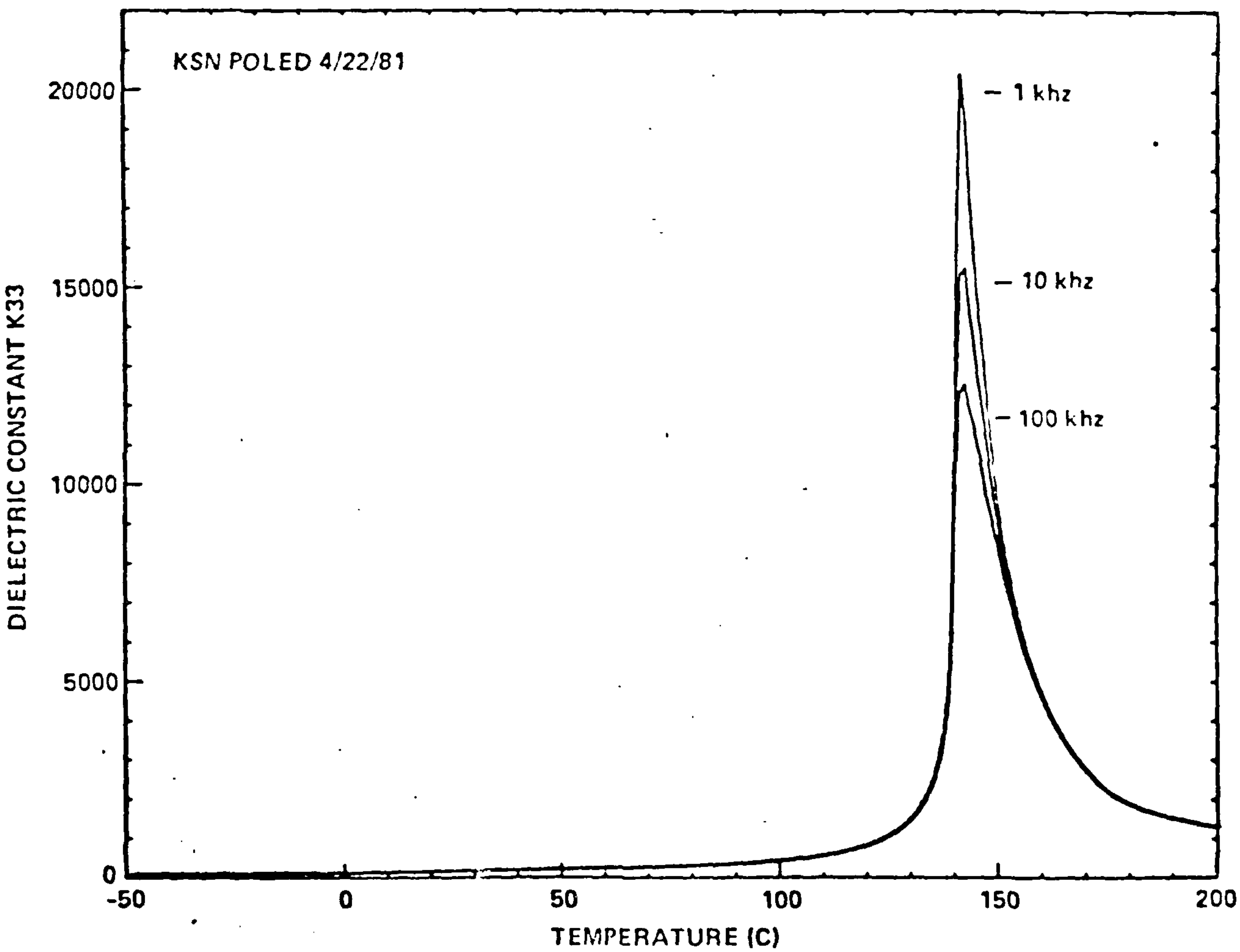

Temperature dependence of dielectric constant (K_{33}) for SKN crystal.

FIGURE 3

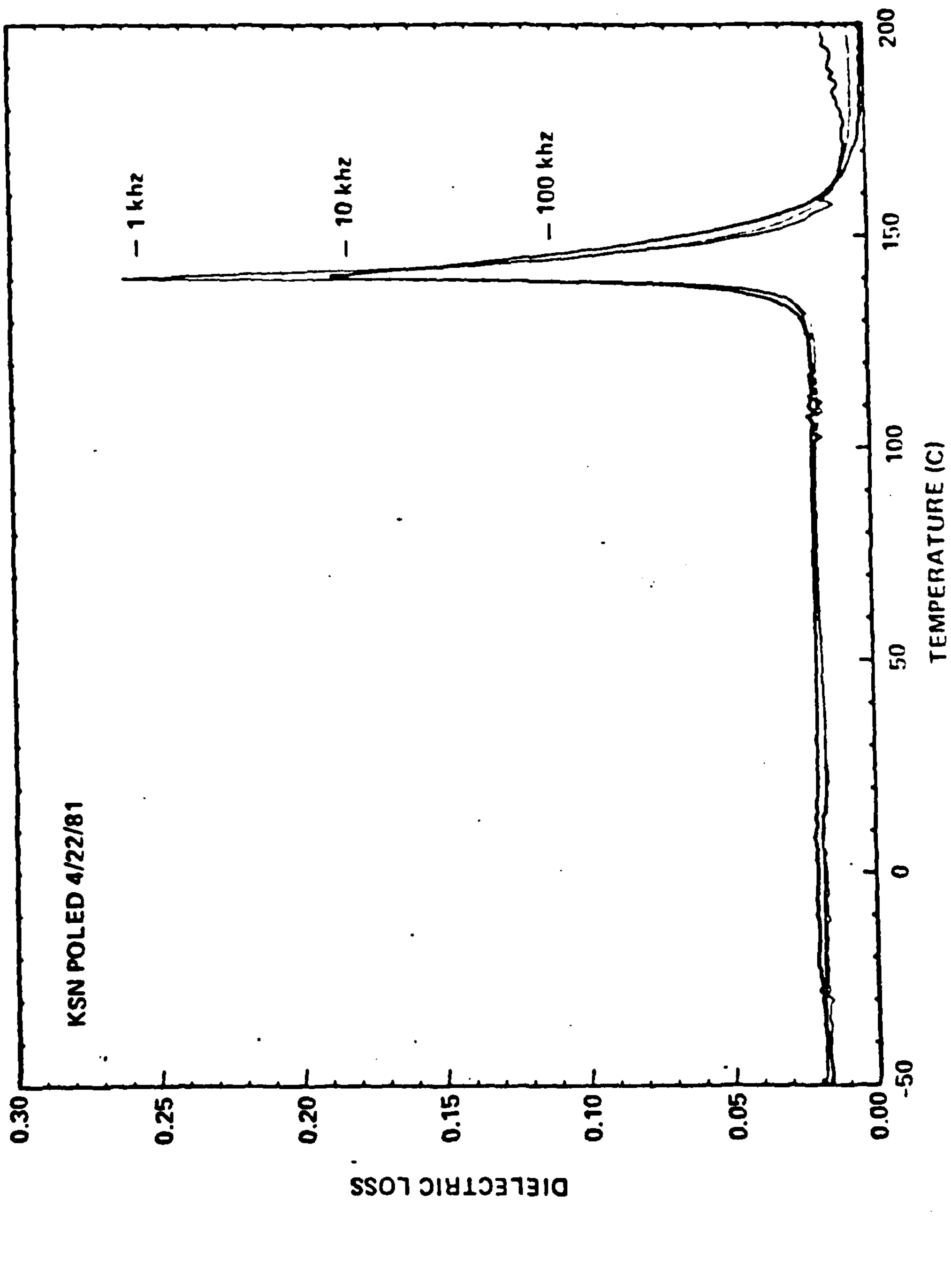

Temperature dependence of dielectric loss of SKN crystals at three frequencies:
1, 10 and 100 KHz.

FIGURE 4

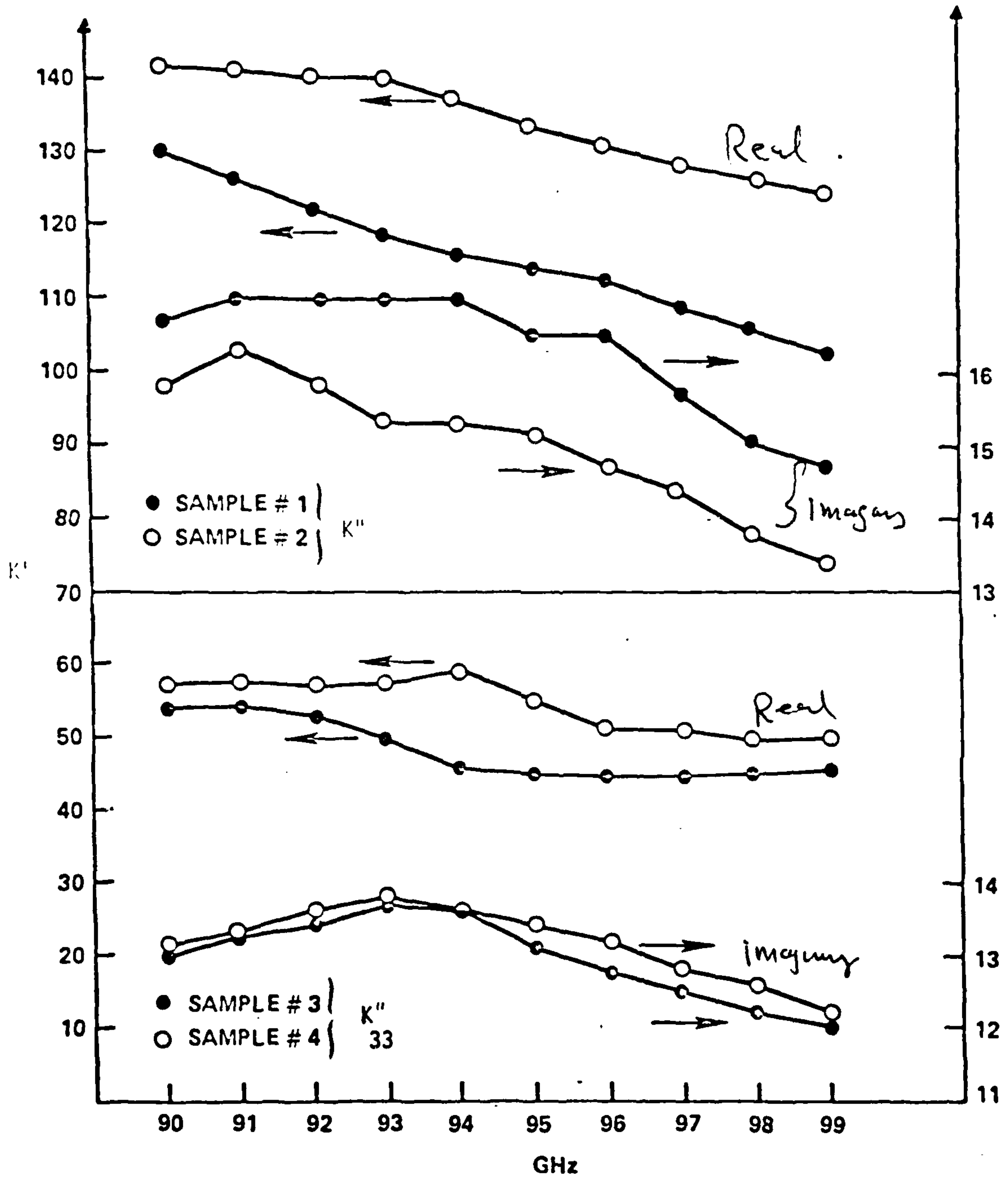

Dielectric properties of SKN single crystal samples for 90-100 GHz.
Top: Real (K') and Imaginary (K") permittivities along crystal a-axis.
Bottom: Real (K') and Imaginary (K") permittivities along crystal c-axis.

APPENDIX 3

GROWTH AND APPLICATIONS OF FERROELECTRIC TUNGSTEN BRONZE FAMILY CRYSTALS

R.R. Neurgaonkar, W.K. Cory and J.R. Oliver

Ferroelectrics, Vol 51, pp 3-8, 1983

GROWTH AND APPLICATIONS OF FERROELECTRIC TUNGSTEN BRONZE FAMILY CRYSTALS

R.R. Neurgaonkar, W.K. Cory and J.R. Oliver
Rockwell International Science Center
Thousand Oaks, CA 91360

Abstract Single crystal growth of several ferroelectric tungsten bronze compositions such as $Sr_{1-x}Ba_xNb_2O_6$ (SBN), $Sr_2KNb_5O_{15}$ (SKN), $Ba_{2-x}Sr_xK_{1-y}Na_yNb_5O_{15}$ (BSKNN) and $K_3Li_2Nb_5O_{15}$ (KLN), has been studied in detail. The results show that the smaller unit cell bronzes, e.g., SBN and SKN, have a cylindrical growth habit with 24 well-defined facets while the larger unit cell bronzes, e.g., BSKNN and KLN, grow in a square shape with 4 well-defined facets. Significant changes in the dielectric and piezoelectric properties can be obtained with changes in composition, and significant differences in the physical properties, e.g., k_{33}, d_{33} and d_{15}, can be observed between the small and large unit cell bronzes.

INTRODUCTION

Single crystal ferroelectric tungsten bronzes in general are known for their excellent electro-optic,[1,2] pyroelectric[3] and piezoelectric[4] properties, making them promising candidates for use in various device applications such as laser modulators, pyroelectric infrared detectors, SAW and other ferroelectric based devices. This, plus the fact that there are over 150 individual end member bronze compositions with numerous possible solid solutions,[5] makes the tungsten bronze family one of the most extensive, versatile and potentially useful families of oxygen octahedra based ferroelectrics.

Typically, the bronze ferroelectrics which are of most practical interest are ones of complex composition and/or solid solutions which are inherently difficult to grow in single crystal form. In the present paper, we report the bulk single crystal growth of various bronze compositions and their possible use in a number of ferroelectric device applications.

EXPERIMENTAL AND DISCUSSION OF RESULTS

Crystal Growth

The materials used for growth were specpure $SrCO_3$, $BaCO_3$, PbO, K_2CO_3, Li_2CO_3, Na_2CO_3 and Nb_2O_5. Table I summarizes the compositions of the individual crystals and their growth conditions. The starting materials were weighed out according to the stoichiometry and then ball-milled in acetone for 10-15 hrs. The resulting slurry was air dried and then fired in a platinum dish at 1000°-1300° for 24 hrs. The furnace was R.F. induction heated and the crystals were grown by the Czochralski technique. The crystal growth procedure for the bronze crystals has been discussed in our earlier paper.[6]

TABLE I Czochralski growth data for tetragonal tungsten bronze compositions.

Composition	Growth Temperature (°C)	Growth Direction	Growth Habit	Crystal Diameter (cm)	Remarks
$Sr_{0.6}Ba_{0.4}Nb_2O_6$	1510	(001)	Cylindrical	~ 3.0	Crack-free and excellent quality
$Sr_{0.5}Ba_{0.5}Nb_2O_6$*	1500	(001)	Cylindrical	~ 1.8 to 2.0	Moderate quality
$Ba_{2-x}Sr_xK_{1-y}Na_yNb_5O_{15}$	1480	(001)	Square	~ 0.8 to 1.0	Crack-free and good quality
$Sr_2KNb_5O_{15}$**	1480	(001)	Cylindrical	~ 0.5 to 0.8	Moderate quality
$K_3Li_2Nb_5O_{15}$**	1050	(001)	Square	0.3 to 0.5	Cracks
		(100)	Square	0.5 to 0.8	Crack-free, reasonable quality
		(110)	Square	0.5 to 0.8	Crack-free, reasonable quality
$K_3Li_2Nb_{5-x}Ta_xO_{15}$	1000-1250	(001) (110)	Square	0.5 to 1.0	Reasonable quality with excellent properties
$Pb_{0.33}Ba_{0.70}Nb_{1.987}O_6$***	~ 1350	(001)		0.8 to 1.0	Few cracks, but excellent properties

*Non-congruent melting composition
**Difficult to grow
***Grown at Penn State, difficult to grow.

Since all of the compositions selected in this investigation are typically solution systems, single crystal growth by the Czochralski technique was found to be difficult, particularly for K^{+}- and Na^{+} containing bronze compositions. The growth problems can be briefly summarized as follows:

- Solid solution systems: difficult to determine the true congruent melting composition, hence optical striation problems.
- Container and contamination, specifically when an iridium crucible is used.
- Cracking of crystals when cycling through the paraelectric/ferroelectric phase transition temperature.

Single crystal growth of the bronze compositions SBN:60 and SBN:50 is relatively easier as compared to the other bronze compositions in this study, with crystals as large as 2 to 3 cm in diameter being successfully grown. Although SBN:60 is the only congruent melting composition in the $SrNb_2O_6$-$BaNb_2O_6$ system, initially coring was a severe problem in this crystal, as well as in the other bronze crystals. This problem has been substantially minimized by maintaining better temperature stability and withdrawing the crystals at a composition as close to the congruent melt as possible. The growth of K^{+}- and Na^{+}-containing solid solution crystals was found to be difficult due to a lack of information on the true congruent melting compositions, and it was also found difficult to properly control the thermal gradients near the solid-liquid interface during growth. In spite of these difficulties, we have been successful in growing BSKNN, SKN and KLN crystals of approximately 1 cm in diameter and several centimeters long.

The cracking problem in bronze crystals, particularly in the K^+- and Na^+-containing bronzes, has been shown to be related to the c-axis dimensional change as the crystal is cooled through the paraelectric/ferroelectric phase transition temperature. In crystals grown from melts containing K^+, Na^+ or Nb_2O_5, the change in the lattice dimensions as a function of temperature is not only much less pronounced than in crystals grown from stoichiometric melts, but the change also takes place at lower temperatures as result of the depression in the Curie temperature. Both these effects make the crystals much more resistant to thermal shock and resultant cracking.

Ferroelectric Properties of Bronze Crystals

Optically, the bronze crystals appear to be of excellent quality and are clear and transparent. Except for BSKNN, all other crystals are pale to dark yellow in color, depending on the crystal diameter. Most of the BSKNN crystals are colorless. Crystals grown along the c-axis are usually well faceted, which is quite exceptional for Czochralski-grown crystals. The smaller unit cell bronzes, e.g., SBN and SKN, are cylindrical in shape and exhibit 24 well-defined facets,[7] while the larger unit cell bronzes are square in shape and show 4 well-defined facets.[8] Figure 1 shows the idealized forms for these crystals. This is a unique advantage for this family, since it can significantly ease the task of crystal orientation.

Because of the large number of parameters needed to fully characterize the system (4 mm), which includes six elastic, three piezoelectric and two dielectric constants, several specimens with various shapes and orientations (001, 100, 110, etc.) have been used. Prior to measurement, the crystals were poled by field-cooling with a dc field of 5-6 KV/cm along the (001) direction. Table II summarizes the measured ferroelectric properties of the various bronze crystals grown in this study.

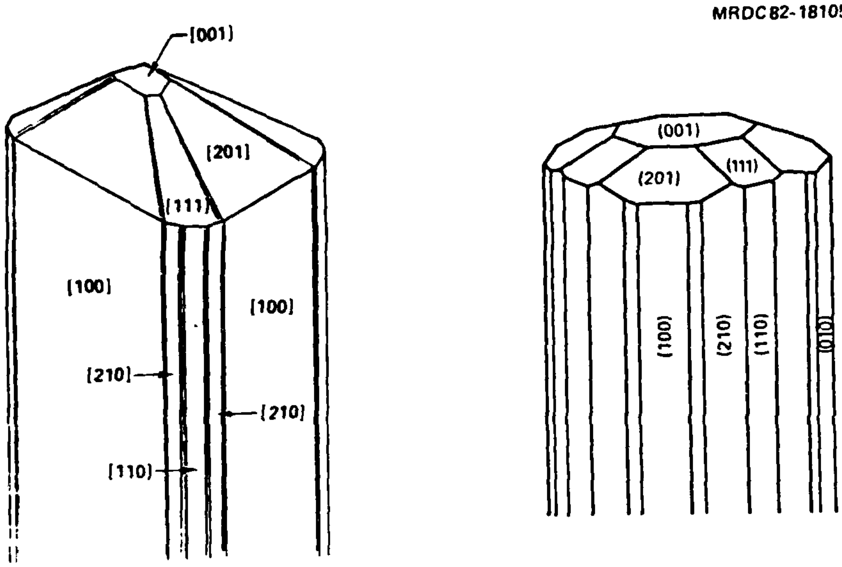

BIGGER UNIT CELL T.B. CRYSTALS SMALLER UNIT CELL T. B. CRYSTALS

FIGURE 1 Idealized forms of tungsten bronze crystals.

TABLE II Physical properties of bronze crystals at room temperature.

Property	SBN:60	SBN:50	BSKNN	SKN	KLN
Lattice Constants	a = 12.462Å c = 3.938Å	a = 12.480Å c = 3.952Å	a = 12.506Å c = 3.962Å	a = 12.470Å c = 3.942Å	a = 12.590Å c = 4.015Å
Curie Temperature (°C)	72°C	125°C	203°C	15[illegible]°C	405°C
Dielectric Constant	ϵ_{33} = 880	ϵ_{33} = 500	ϵ_{33} = 420	ϵ_{33} = 120[illegible]	ϵ_{33} = 12[illegible]
Electromechanical Coupling Coefficients	k_{33} = 0.47 k_{31} = 0.14 k_{15} = 0.24	k_{33} = 0.48 k_{31} = 0.137 k_{15} = ---	k_{33} = 0.47 k_{31} = --- k_{15} = 0.28	k_{33} = 0.44 k_{31} = --- k_{15} = 0.26	k_{33} = 0.52 k_{31} = 0.-- k_{15} = 0.36
Piezoelectric Constants ($\times 10^{12}$ C/N)	d_{33} = 130 d_{15} = 31	d_{33} = 100 d_{15} = 24	d_{33} = 60 d_{15} = 80	- -	d_{33} = 57 d_{15} = 68
Electro-Optic Coefficient (M/V)	420×10^{-12}	180×10^{-12}	360×10^{-12}	160×10^{-12}	60×10^{-12}

All crystals exhibit room temperature tetragonal bronze structure (4 mm).

These data clearly indicate that the room temperature dielectric, piezoelectric and electromechanical coupling constants of these crystals are excellent, making them of great interest for a variety of ferroelectric devices.

The intetesting feature of these measurements is that the piezoelectric strain coefficients d_{33} and d_{15} are significantly different between the smaller and larger unit cell bronzes. For example, d_{33} is relatively large for the smaller unit cell crystals while d_{15} is large for the bigger unit cell crystals. Further investigation is in progress to establish the major differences in the physical properties between small and large unit cell bronzes. Once such data is established, the selection of bronze crystals for a given device application will be significantly easier.

ACKNOWLEDGMENT

This research was supported by various agencies, including DARPA, ONR and AFOSR.

REFERENCES

1. H. Hirano, H. Takei and S. Koide, Jap J. Appl. Phys., 8, 972 (1969).
2. P.V. Lenzo, E.G. Spencer and A.A. Ballman, Appl. Phys. Let. 11, 23 (1967).
3. A.M. Glass, J. Phys. 40, 4699 (1969).
4. Landolt-Bornstein, Ferroelectrics and Related Substances, New Series, 16 (1981).
5. E.C. Subbarao, G. Shirane and F. Jona, Acta. Cryst. 13, 226 (1960).
6. R.R. Neurgaonkar, M.H. Kalisher, T.C. Lim, E.J. Staples and K.L. Keester, Mat. Res. Bull. 15, 1235 (1980).
7. O.F. Dudnik, A.K. Gromov, V.B. Kravchenko, Y.L. Kopylov and G.F. Kunznetsov, Sov. Phys. Crystagraph. 15, 330 (1970).
8. T. Fukuda, H. Hirano and S. Koide, J. Cryst. Growth 6. 293 (1970).

APPENDIX 4

FERROELECTRIC PROPERTIES OF TETRAGONAL TUNGSTEN BRONZE SINGLE CRYTALS

R.R. Neurgaonkar, J.R. Oliver and L.E. Cross

Ferroelectrics, Vol. 56, pp 31-36, 1984

FERROELECTRIC PROPERTIES OF TETRAGONAL TUNGSTEN BRONZE SINGLE CRYSTALS

R.R. NEURGAONKAR AND J.R. OLIVER
Rockwell International Science Center,
Thousand Oaks, CA 91360, USA

and

L.E. CROSS
Pennsylvania State University,
University Park, PA 16802, USA

Abstract Ferroelectric tetragonal tungsten bronze (T.B.) family single crystals, e.g., SBN, BSKNN, KLN, SKN and PBN, have been grown and their ferroelectric properties have been investigated. The results show that the dielectric, piezoelectric, and electromechanical coupling coefficients are significantly large for these crystals; however, they are markedly different when going from smaller to bigger unit cell T.B. crystals. For example, ε_{33} and d_{33} are substantially larger for the smaller unit cell T.B. crystals, e.g., SBN and SKN, while ε_{11} and d_{15} are dominant for bigger unit cell bronzes. However, these differences do not have such a significant effect on the respective electro-optic and pyroelectric properties.

INTRODUCTION

Tungsten bronze (T.B.) family crystals exhibit interesting electro-optic, nonlinear-optic and pyroelectric properties and these attractive features make them potentially important for applications in optoelectronics. However, up to the present time these applications have been limited by the difficulty of growing large single crystals having good optical homogeneity. Recently, Neurgaonkar et al[1-4] and Shrout et al[5] studied the problems associated with the Czochralski crystal growth technique and successfully developed the technique for various T.B. crystals, e.g., $Sr_{1-x}Ba_xNb_2O_6$ (SBN), $Ba_{2-x}Sr_xK_{1-y}Na_yNb_5O_{15}$ (BSKNN), $K_3Li_2Nb_5O_{15}$ (KLN), $Sr_2KNb_5O_{15}$ (SKN) and $Pb_{1-x}Ba_xNb_2O_6$ (PBN). This now makes it possible to study the ferroelectric, electro-optic and other properties of these compositions for various potential device applications. The present paper reports on the compositional and temperature dependence of the ferroelectric properties for several of these T.B. crystals.

RESULTS AND DISCUSSION

Materials Preparation

All tetragonal tungsten bronze crystals studied in the present work were grown by the Czochralski technique established at Rockwell International. The problems associated with this technique and their important features have been described in earlier publications.[1-5] The bronze crystals grown along the c-axis are usually faceted, which is quite exceptional for Czochralski-grown crystals. The interesting feature in this family is that the smaller unit cell crystals, e.g., SBN and SKN, grow in a cylindrical shape with 24 well-defined facets, while the bigger unit cell bronze crystals such as BSKNN, KLN and PBN grow in a square shape with 4 well-defined facets.[3]

Sample Preparation

Because of the large number of parameters needed to fully characterize the tetragonal (4 mm) bronze crystals, which include two dielectric, three piezoelectric and six elastic constants, several specimens with various shapes and orientations were used in the present investigation (Figure 1). Prior to measurement, the crystals were poled by the field-cooling method under a field of 5-8 kV/cm along the c-axis. The measurement techniques used to evaluate the temperature dependence of the dielectric, piezoelectric, elastic and other important coefficients have been described by Shrout et al.[6]

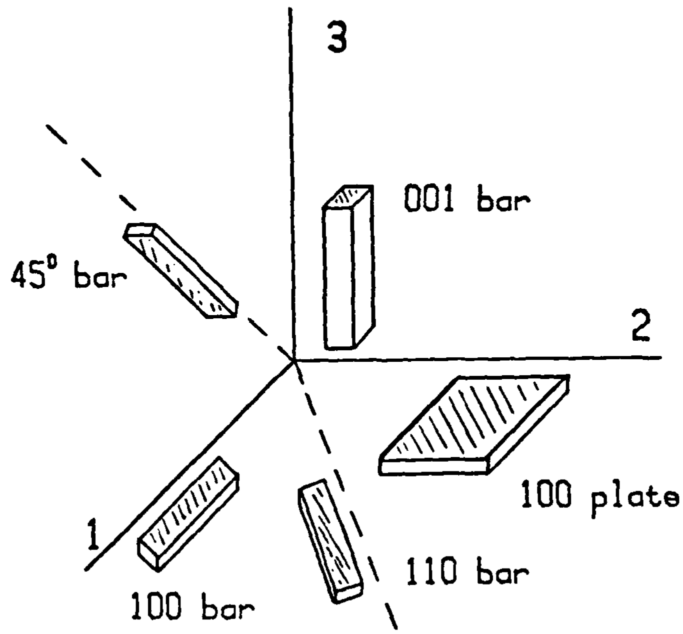

FIGURE 1 Shape and orientations of specimens.

Ferroelectric Characteristics of Bronze Crystals

Table I summarizes the results of measurements including structural, ferroelectric and electro-optic, for these selected bronze crystals. The temperature dependence of the dielectric constants ε_{33} and ε_{11} and the dielectric loss (tan δ) were determined from (001) and (100) plates at frequencies of 1, 10, 100 and 1000 KHz. The temperature range covered was 20° to 500°C, depending upon the Curie temperature, T_c, for the given crystal. Both ε_{33} and ε_{11} showed marked anomalies at the transition point. The general temperature behavior and large anisotropy of ε_{33} and ε_{11} is typical of all the bronze crystals. However, the magnitude of dielectric constant is markedly different for each composition, and seems to depend strongly on the size of the unit cell of the given bronze crystal. For example, ε_{33} is large while ε_{11} is small for the smaller unit cell bronzes, e.g., SBN and

SKN. On the other hand, the situation is reversed in the case of bigger unit cell bronzes where ε_{33} is smaller while ε_{11} is larger. The dielectric properties were further studied by cooling below room temperature, and it was found that in the case of bigger unit cell bronzes the dielectric constant ε_{11} increased with decreasing temperature, indicating the presence of another ferroelectric-ferroelectric phase transition. This type of behavior has also been observed for another bronze crystal, $Ba_2NaNb_5O_{15}$, by Toledano et al.[7] Further work is in progress on BSKNN, KLN and PBN crystals to establish the existence of the low temperature transition. In general the dielectric loss for these crystals is low, on the order of 0.03 or less at room temperature.

TABLE I Ferroelectric and structural properties of tetragonal bronze crystals at room temperature.

	$Sr_{0.6}Ba_{0.4}Nb_2O_6$	$Sr_2KNb_5O_{15}$	BSKNN*	$K_3Li_2Nb_5O_{15}$	$Pb_{0.24}Ba_{0.69}Nb_2O_6$
Unit Cell Dimensions	a = 12.462Å c = 3.938Å	a = 12.470Å c = 3.942Å	a = 12.506Å c = 3.982Å	a = 12.590Å c = 4.015Å	a = 12.510Å c = 3.995Å
Curie Temp (°C)	72	150	203	405	350
Dielectric Constant, after poling, at 23°C	ε_{33} = 470 ε_{11} = 204	ε_{33} = 760 ε_{11} = 750	ε_{33} = 180 ε_{11} = 380	ε_{33} = 115 ε_{11} = 308	ε_{33} = 140 ε_{11} = 350
Piezoelectric Constant (10^{-12} C/N)	d_{33} = 130 d_{15} = 31	— —	d_{33} = 60 d_{15} = 70	d_{33} = 57 d_{15} = 68	d_{33} = 40 d_{15} = 70
SAW Electromechanical Couling Constant, K^2	180×10^{-4}	90×10^{-4}	—	—	—
Pyroelectric Coefficient C/km^2	850×10^{-12}	650×10^{-12}	440×10^{-12}	—	180×10^{-12}
Electro-Optic Coefficient, r_{33} (m/V)	420×10^{-12}	160×10^{-12}	200×10^{-12}	60×10^{-12}	—
Electro-mechanical Coupling Coefficients	K_{33} = 0.47 K_{15} = 0.24	K_{33} = 0.44 K_{15} = 0.26	K_{33} = 0.46 K_{15} = 0.38	K_{33} = 0.52 K_{15} = 0.36	— —
Spontaneous Polarization, P_s (C/m^2)	0.65	—	—	0.25	0.40

*BSKNN - $B_{1.2}Sr_{0.8}K_{0.75}Na_{0.25}Nb_5O_{15}$.

As summarized in Table I, the electro-optic (r_{33}) and pyroelectric (p_{33}) coefficients are large and appear to be less affected when going from smaller to bigger unit cell T.B. crystals. These results are interesting, and further work is in progress to examine the correlation of these characteristics with the piezoelectric and dielectric properties. At the present time, both SBN and BSKNN crystals exhibit the optimum electro-optic and pyroelectric properties from each classification, and are now being studied in more detail.

The surface acoustic wave (SAW) coupling constant K^2 for $Sr_{0.6}Ba_{0.4}Nb_2O_6$ (SBN:60) crystals has been shown to be large for the (001)-plane propagating along the (100) direction; its value is measured to be 180×10^{-4}, which is comparable to the best known bronze crystal, $Pb_2KNb_5O_{15}$ (188×10^{-4}). Furthermore, both SBN:60 and $Pb_2KNb_5O_{15}$ crystals show temperature compensated cuts, and this opens up exciting opportunities for the use of these crystals in SAW device applications.

Table II summarizes the classification of T.B. crystals based on unit cell dimensions, growth habits and ferroelectric properties. It is hoped that this classification will be found useful for future work in the selection of proper bronze compositions for new device applications.

TABLE II Classification of tungsten bronze family.

TABLE II. Classification of tungsten bronze family.

T.B. Compositions with Smaller Unit Cell Dimensions (e.g., $Sr_{1-x}Ba_xNb_2O_6$, $Sr_2KNb_5O_{15}$ $Sr_2NaNb_5O_{15}$, etc.)	T.B. Compositions with Bigger Unit Cell Dimensions (e.g., $Ba_{2-x}Sr_xK_{1-y}Na_yNb_5O_{15}$, $Pb_{1-x}Ba_xNb_2O_6$, $K_3Li_2Nb_5O_{15}$, etc.)
• Crystal habit is cylindrical with 24 defined facets	• Crystal habit is square with 4 defined facets
• Relatively low T_c, below 200°C	• Moderately high T_c, above 200°C
• Relatively high dielectric constant (ϵ_{33} high at room temperature)	• Moderately high dielectric constant (ϵ_{11} high at room temperature)
• High piezoelectric coefficient d_{33}, but low d_{15}, at room temperature	• High piezoelectric coefficient d_{15}, but low d_{33}, at room temperature
• High electro-optic and pyroelectric coefficients	• Moderately high electro-optic and pyroelectric coefficients
• Large excellent quality crystals available (2 to 3 cm diameter)	• Moderately large crystals available (1 to 1.5 cm diameter)

ACKNOWLEDGMENT

This research was supported by various agencies, including DARPA, ONR and AFOSR.

REFERENCES

1. R.R. Neurgaonkar, W.K. Cory and J.R. Oliver, accepted for publication in Ferroelectrics.
2. R.R.Neurgaonkar, M.H. Kalisher, T.C. Lim, E.J. Staples and K.L. Keester, Mat. Res. Bull. 15, 1305, (1980).
3. R.R. Neurgaonkar, W.K. Cory, W.W. Ho and L.E. Cross, Ferroelectrics, 38, 857, (1981).
4. R.R. Neurgaonkar, W.K. Cory, J.R. Oliver and L.E. Cross, private communication.
5. T.R. Shrout, L.E. Cross and D.A. Hukin, accepted for publication in Ferroelectrics.
6. T.R. Shrout, L.E. Cross, P. Moses, H.A. McKinstry and R.R. Neurgaonkar, Proceedings of the IEEE Ultrasonics Symposium, 414, (1980).
7. J.C. Toledano, Ann. Telec, 29, 249, (1974).

Rockwell International
Science Center

SC5345.4AR

APPENDIX 5

STRUCTURAL AND DIELECTRIC PROPERTIES OF THE PHASE
$Pb_{1-2x}K_xM_x^{3+}Nb_2O_6$, M = La or Bi

R.R. Neurgaonkar, J.R. Oliver, W.K. Cory and L.E. Cross
Mat. Res. Bull. Vol. 18, pp 735-741, 1983

Rockwell International
Science Center

STRUCTURAL AND DIELECTRIC PROPERTIES OF THE PHASE $Pb_{1-2x}K_xM_x^{3+}Nb_2O_6$, M = La or Bi

R.R. Neurgaonkar, J.R. Oliver and W.K. Cory
Rockwell International Science Center
Thousand Oaks, CA 91360

and

L.E. Cross
Materials Research Laboratory
Pennsylvania State University
University Park, PA 16802

ABSTRACT

The $Pb_{1-2x}K_xM_x^{3+}Nb_2O_6$, M = La or Bi, solid solutions have been prepared by solid state reaction and their structural and ferroelectric properties have been established. Complete crystalline solid solubility exists in both systems; in addition, three structurally related phases, namely, the ferroelectric orthorhombic and tetragonal tungsten bronze phases and the paraelectric tetragonal $K_{.5}La_{.5}Nb_2O_6$ type phase, have been identified at room temperature. The composition ranges for three phases are $0.0 < x \sim 0.47$, $0.48 \sim x \sim 0.85$, $0.86 \sim x \sim 1.0$, respectively. The ferroelectric phase transition temperature, T_c, decreases with increasing concentration of K^+ and La^{3+} or Bi^{3+} in the orthorhombic tungsten bronze phase. A few compositions from each system exhibit excellent dielectric and piezoelectric characteristics, indicating that they could be future materials for piezoelectric and high frequency dielectric studies.

INTRODUCTION

Lead metaniobate, $PbNb_2O_6$, was first studied and reported ferroelectric by Goodman in 1953;[1,2] since then, this material has been the subject of several investigations. Although the curie temperature was much higher than that of any known ferroelectric, the material did not find immediate application because of the difficulty in preparing good nonporous ceramics and the associated problem of poling them. By analogy with previous work on barium titanate and other ferroelectric hosts, the effect of replacing part of the Pb^{2+} by other divalent and trivalent ions[3-13] or Nb^{5+} by tretravalent or hexavalent ions was studied, with the objective of improving the sintering and general ferroelectric properties of ceramics. It was reported that the curie temperature was reduced, and although this would be a disadvantage, this made it possible to pole the material more effectively and successfully enhance the dielectric and piezoelectric properties.

Since our current interest is in millimeter wave device applications, the search for a suitable ferroelectric material having strong dielectric and piezoelectric properties is constantly being made. The present work reports the structural, dielectric and piezoelectric properties of the solid solutions based on the $PbNb_2O_6$ phase, i.e., $Pb_{1-2x}K_xM_x^{3+}Nb_2O_6$, where M = La or Bi.

EXPERIMENTAL PROCEDURE

PbO, K_2CO_3 (Baker Analyzed Grade), Bi_2O_3 (Fischer Scientific Co.), La_2O_3 (American Potash and Chem. Corp.), and Nb_2O_5 (Atomergic Co.) were used as the starting materials. The ceramic specimens were prepared by the conventional technique of milling, prefiring, crushing, pressing and firing. The specimens were prepared in the form of disks 1.3 cm in diameter and 0.3 cm thick. The final sintering was for 2-3 hours, and the temperature, which depended on composition, was between 1250°C-1300°C.

Preparation of pure $PbNb_2O_6$ is complicated by the existence of ferroelectric and nonferroelectric modifications.[1,2] The transition between these modifications is reversible, although it is accompanied by considerable temperature hystersis. The high temperature ferroelectric form was prepared by heating to 1320°C for 30 minutes and then cooling rapidly. X-ray powder diffraction data was obtained with a Norelco diffractometer using CuK radiation and a graphite monochromator operating at 35 kV and 28 ma. Measurements were made from strip charts produced by scanning 1/4 2o/min on acetone smear-mounted powders. The measurements are believed to be accurate to ±0.02 2o. Instrumental error was corrected through the use of an internal silicon standard. Least-squares analysis of the data for refined cell constants was performed on a Harris Model 1660 computer.

The fired disks were metalized on the major surfaces by using either platinum paste or a vacuum-deposited layer of platinum. Disks required to be poled were heated in silicone oil, and a static field of 20 kV per cm was applied at temperatures as near as possible to 150°C to 170°C, the field being maintained while the disks were allowed to cool.

CRYSTALLINE SOLUBILITY AND STRUCTURAL TRANSITIONS

The work on $K_{.5}La_{.5}Nb_2O_6$ by Soboleva and Dmitrieva[14] and our work on $K_{.5}Bi_{.5}Nb_2O_6$ show that these two phases crystallize in the tetragonal crystal symmetry, and are isostructural with high temperature tetragonal modification of $PbTa_2O_6$. At room temperature, the ferroelectric $PbTa_2O_6$ phase has an orthorhombic symmetry and is isostructural with the tungsten bronze $PbNb_2O_6$ phase. This suggests that all the systems considered in this work are structurally related and should form a continuous solid solution in the pseudo-binary systems, $PbNb_2O_6$-$K_{.5}La_{.5}Nb_2O_6$ and $PbNb_2O_6$-$K_{.5}Bi_{.5}Nb_2O_6$. The results of x-ray diffraction powder work are in good agreement, and a complete solid solution has been identified in both of the systems. Three structurally related phases, namely, the orthorhombic and tetragonal tungsten bronze type phases and the tetragonal $K_{.5}La_{.5}Nb_2O_6$ have been established for the $Pb_{1-2x}K_xM_x^{3+}Nb_2O_6$, M = La or Bi, solid solution system. Figure 1 shows x-ray diffraction powder patterns for the three phases.

The results of x-ray measurements at room temperature show a homogeneity range of the orthorhombic tungsten bronze phase to $x = 0.47$, while the tetragonal tungsten bronze phase is present in the composition range $0.48 < x < 0.85$. At the other end, the crystalline solid solubility of $PbNb_2O_6$ in the $K_{.5}M_x^{3+}Nb_2O_6$ phase is limited, and is estimated to be in the composition range $0.86 < x < 1.0$. At composition $x = 0.47$, both the orthorhombic and tetragonal tungsten bronze phases coexist. This type of morphotropic condition has also been reported on the $Pb_{1x}Ba_xNb_2O_6$ system.[3,10] The variation of lattice parameters as a function of composition for the system $Pb_{1-2x}K_xLaNb_2O_6$ is shown in Fig. 2. The a and c parameters increased only slightly, while the b parameter decreased considerably with increasing concentration of $k_{.5}M_{.5}^{3+}Nb_2O_6$ in the $PbNb_2O_6$ phase. The decrease in the b parameter was substantial compared to the a parameter, so that the ratio a/b becomes close to unity for values $x > 0.50$.

FERROELECTRIC DATA

The curie temperature, T_C, is known to be one of the fundamental characteristics of ferro and antiferroelectrics. This measurement gives the origin of the spontaneous polarized state and is considered important for characterizing piezoelectric materials. In the present work, T_C for the different solid solution systems has been obtained by measuring the dielectric properties as a function of temperature. The technique is relatively simple, and the measurements have been routinely made by using a capacitance bridge (HP 4270A). The test specimens (disks) used for the dielectric measurements are approximately 1.3 cm in diameter and 0.3 cm thick, and are coated on each side with platinum by the standard vacuum evaporation technique.

A typical plot of the dielectric constant vs temperature is given in Fig. 3 for a few compositions on the $Pb_{1-2x}K_xLa_xNb_2O_6$ system. It can be seen that the dielectric constant decreases and broadens, whereas the room temperature dielectric constant increases with increasing K^+ and La^{3+} or Bi^{3+} up to x = 0.40. Furthermore, the ferroelectric phase transition temperature, T_c, is shifted towards a lower temperature with increasing amounts of $K_{.5}La_{.5}Nb_2O_6$ in $PbNb_2O_6$. T_c for the pure $PbNb_2O_6$ has been recorded at 560°C,[1,2] and this temperature dropped with the addition of K^+ and La^{3+} or Bi^{3+} in both the orthorhombic and the tetragonal tungsten bronze phases. By using this peak position, the transition temperature for each system has been determined. Figure 4 shows the variation of T_c as a function of composition for the $Pb_{1-2x}K_xLa_xNb_2O_6$ and $Pb_{1-2x}K_xBi_xNb_2O_6$ systems. Variations of T_c with composition is linear in both systems and is approximately of the same order. Lowering of T_c has also been reported for several other systems based on the $PbNb_2O_6$ solid solutions.[4,7-12]

Table 1 summarizes the physical constants for the $Pb_{1-2x}K_xLa_xNb_2O_6$ and $Pb_{1-2x}K_xBi_xNb_2O_6$ systems. As can be seen from this data, the dielectric constant has increased significantly with the addition of K^+ and La^{3+} or Bi^{3+} in the orthorhombic tungsten bronze phase with the composition $Pb_{.8}K_{.1}La_{.1}Nb_2O_6$ and $Pb_{.7}K_{.15}Bi_{.15}Nb_2O_6$ exhibiting the optimum dielectric constant for each system. The piezoelectric strain coefficient (d_{33}) measurements on various samples were performed using the Berlincourt d_{33} meter, and the results of this study indicate that the composition $Pb_{.8}K_{.1}La_{.1}Nb_2O_6$ again shows the optimum d_{33} coefficient for these systems. We believe these values may increase substantially if the poling is achieved at higher temperature. In the present case, the poling was accomplished in a silicone oil bath at approximately 150°C, which is a very low temperature compared to the respective curie temperatures. It is anticipated that by improving the poling technique for these ceramic samples, it will be possible to better establish the d_{33} coefficient. In any case, the present piezoelectric strain coefficient value obtained for the $Pb_{.8}K_{.1}La_{.1}Nb_2O_6$ sample is much higher than that reported[6] for the $PbNb_2O_6$ crystal, indicating that these compositions can find use for piezoelectric transducer and high frequency dielectric applications.

The effect of a variety of different substituent ions, such as Ba^{2+}, Sr^{2+}, Ca^{2+}, Cd^{2+} and Bi^{3+} for Pb in the $PbNb_2O_6$ phase, has been studied and reported in the literature.[3-13] Except for Ba^{2+}, all other ions are smaller than Pb^{2+}, and their addition did not alter the orthorhombic crystal symmetry. However, in the case of the $Pb_{1-x}Ba_xNb_2O_6$ solid solution system,[3,10] the substitution of Ba^{2+} (1.50A) for Pb^{2+} (1.32A) first decreases the orthorhombic distortion, and then induces a tetragonal structure with the polar axis along the c rather than along the b axis. Further, the interesting feature in this system is that T_c first decreases in the orthorhombic tungsten bronze phase and then increases in the tetragonal tungsten bronze phase. This is the unique case in the $PbNb_2O_6$-based solid solutions; also, since the average ionic size of K^+ plus La^{3+} (1.355A) and K^+ plus Bi^{3+} (1.34A) is bigger than Pb^{2+}, and since both systems, $Pb_{1-2x}K_xM_x^{3+}Nb_2O_6$, M = La or Bi, and $Pb_{1-x}Ba_xNb_2O_6$, are structurally similar, it was expected that the addition of K^+ with La^{3+} or Bi^{3+} would produce similar results, i.e., first a decrease and then an increase in the T_c. The results of this investigation (Fig. 4) indicate that a continuously decreasing curie temperature occurs with increasing amounts of K^+ plus La^{3+} or K^+ plus Bi^{3+} in both the orthorhombic and tetragonal tungsten bronze phases, indicating that T_c is not only controlled by the size of substituent ions, but its location in the structure is equally important. Since the coordination of Pb^{2+} is 15- and 12-fold in the tungsten bronze structure, there exists three possibilities for each ion in this structure, namely in the 15 or 12, or in both the sites. Neither the work reported in the literature[3-9] nor the results of this investigation are sufficient to establish the site preference or their distribution over the two crystallographic sites. Further work in this direction is of significant interest in the present study in order to establish the site preference for different ions and their influence over the T_c behavior and the ferroelectric properties.

CONCLUSIONS

Structural data indicate that a complete solid solution exists in the system $PbNb_2O_6$-$K_{.5}M^{3+}_{.5}Nb_2O_6$, where M = La or Bi, and three structurally related phases have been reported for these solid solution systems. The addition of K^+ and La^{3+} or Bi^{3+} has enhanced the dielectric and piezoelectric properties for these systems and, specifically, the compositions $Pb_{.9}K_{.05}La_{.05}Nb_2O_6$, $Pb_{.8}K_{.1}La_{.1}Nb_2O_6$ and $Pb_{.7}K_{.15}La_{.15}Nb_2O_6$ appear to be of interest for piezoelectric transducer and high frequency dielectric studies. Further investigations in these systems are in progress using bulk single crystals of selected compositions. These systems are in many ways similar to $Pb_{1-x}Ba_xNb_2O_6$, and are thus expected to provide materials useful for several piezoelectric device applications.

ACKNOWLEDGEMENT

This research work was supported by the ONR and DARPA agencies.

REFERENCES

1. G. Guodman, J. Am. Ceram. Soc. 36, 368 (1953).
2. G. Goodman, Am. Ceram. Bull. 31, 113 (1952).
3. M.H. Francombe, Acta. Cryst. 13, 131 (1960).
4. V.A. Isupov, V.I. Koiakov, Zh. Tekh. Fiz. 28, 2175 (1958).
5. E.G. Bonnikova, I.M. Larionov, N.D. Smazhevskaya and E.G. Glozman, Izv. Akad. Nauk. SSR., Ser. Fiz. 24, 1440 (1960).
6. B. Lewis and L.A. Thomas, Proc. Int'l. Conf. Solid State Phys. Electronics Telecommun., Brussel 4, Pt. 2, 883 (1960).
7. G. Goodman, Am. Ceram. Soc. Bull. 34, No. 4, Program 11, 1955; U.S. Patent 2,805,165, Sept. 3, 1975, filed April 25, 1955.
8. G. Goodman, U.S. Patent 2,729,757, June 3, 1956; filed June 29, 1951.
9. P. Baxter and N.J. Hellicar, J. Am. Ceram. Soc. 43, 578 (1960).
10. E.C. Subbarao, G. Shirane and F. Jona, Acta. Cryst. 13, 226 (1960).
11. E.C. Subbarao, J. Am. Ceram. Soc. 43, 439 (1960).
12. E.C. Subbarao and J. Hrizo, J. Am. Ceram. Soc. 45, 528 (1962).
13. E.C. Subbarao and G. Shirane, J. Chem. Phys. 32, 1846 (1960).
14. L.V. Soboleva and F.I. Dmitrieva, Inorg. Mat. 6, 1761 (1970).

Table 1
Physical Constants for Modified $PbNb_2O_6$

Composition	Symmetry	Curie Temp T_c, °C	Dielectric Constant, K R.T.	T_c	Piezoelectric Strain, Coeff., d_{33} c/n
$PbNb_2O_6$	Orthorhombic	560			100×10^{-12}
$Pb_{.90}K_{.05}La_{.05}Nb_2O_6$	Orthorhombic	455	280	2610	---
$Pb_{.80}K_{.10}La_{.10}Nb_2O_6$	Orthorhombic	339	720	3390	130×10^{-12}
$Pb_{.70}K_{.15}La_{.15}Nb_2O_6$	Orthorhombic	201	790	1600	106×10^{-12}
$Pb_{.60}K_{.20}La_{.20}Nb_2O_6$	Orthorhombic	98	650	830	---
$Pb_{.80}K_{.10}Bi_{.10}Nb_2O_6$	Orthorhombic	342	280	2310	30×10^{-12}
$Pb_{.70}K_{.15}Bi_{.15}Nb_2O_6$	Orthorhombic	211	750	2840	35×10^{-12}
$Pb_{.60}K_{.20}Bi_{.20}Nb_2O_6$	Orthorhombic	105	1390	2380	---

FIGURE CAPTION

Fig. 1 X-ray diffraction powder patterns for $Pb_{1-2x}K_xLa_xNb_2O_6$ solid solution, where m = La or Bi.

Fig. 2 Variation of lattice parameters for the $Pb_{1-2x}K_xLa_xNb_2O_6$ solid solution.

Fig. 3 Dielectric constant vs temperature of $Pb_{1-2x}K_xLa_xNb_2O_6$.

Fig. 4 Variation of ferroelectric transition temperature for the $Pb_{1-2x}K_xM_x^{3+}Nb_2O_6$ system, M = La or Bi.

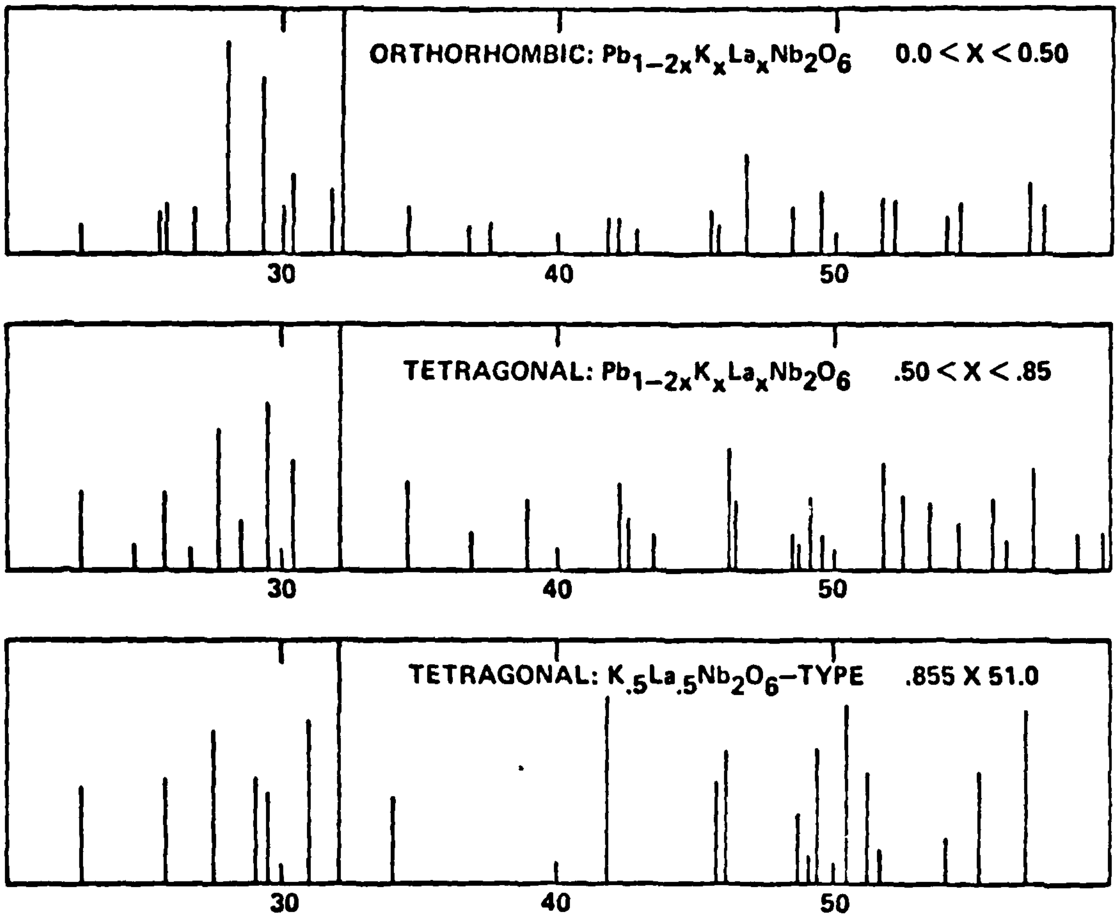
ORTHORHOMBIC: $Pb_{1-2x}K_xLa_xNb_2O_6$ 0.0 < X < 0.50
30
40
50
TETRAGONAL: $Pb_{1-2x}K_xLa_xNb_2O_6$ .50 < X < .85
30
40
50
TETRAGONAL: $K_{.5}La_{.5}Nb_2O_6$–TYPE .855 X 51.0
30
40
50

MRDC81-12758

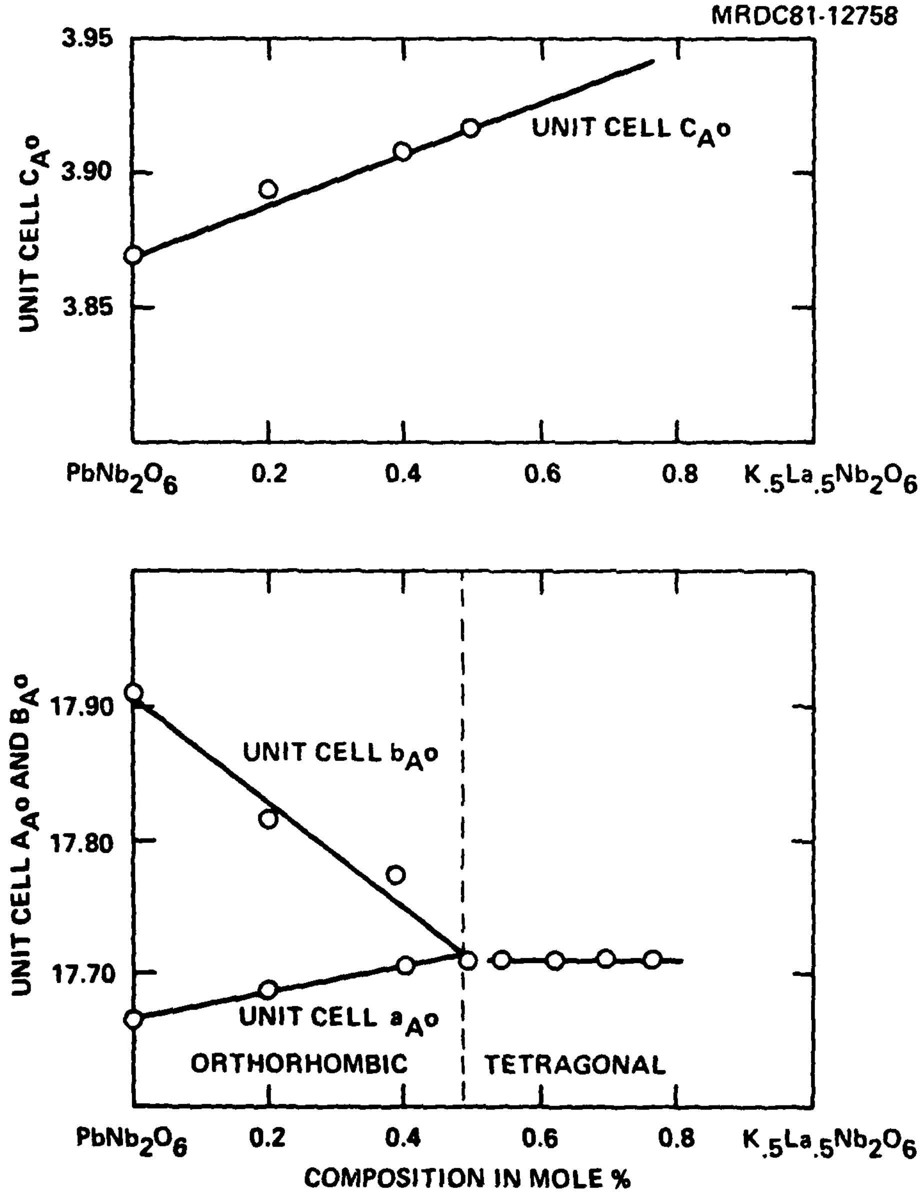

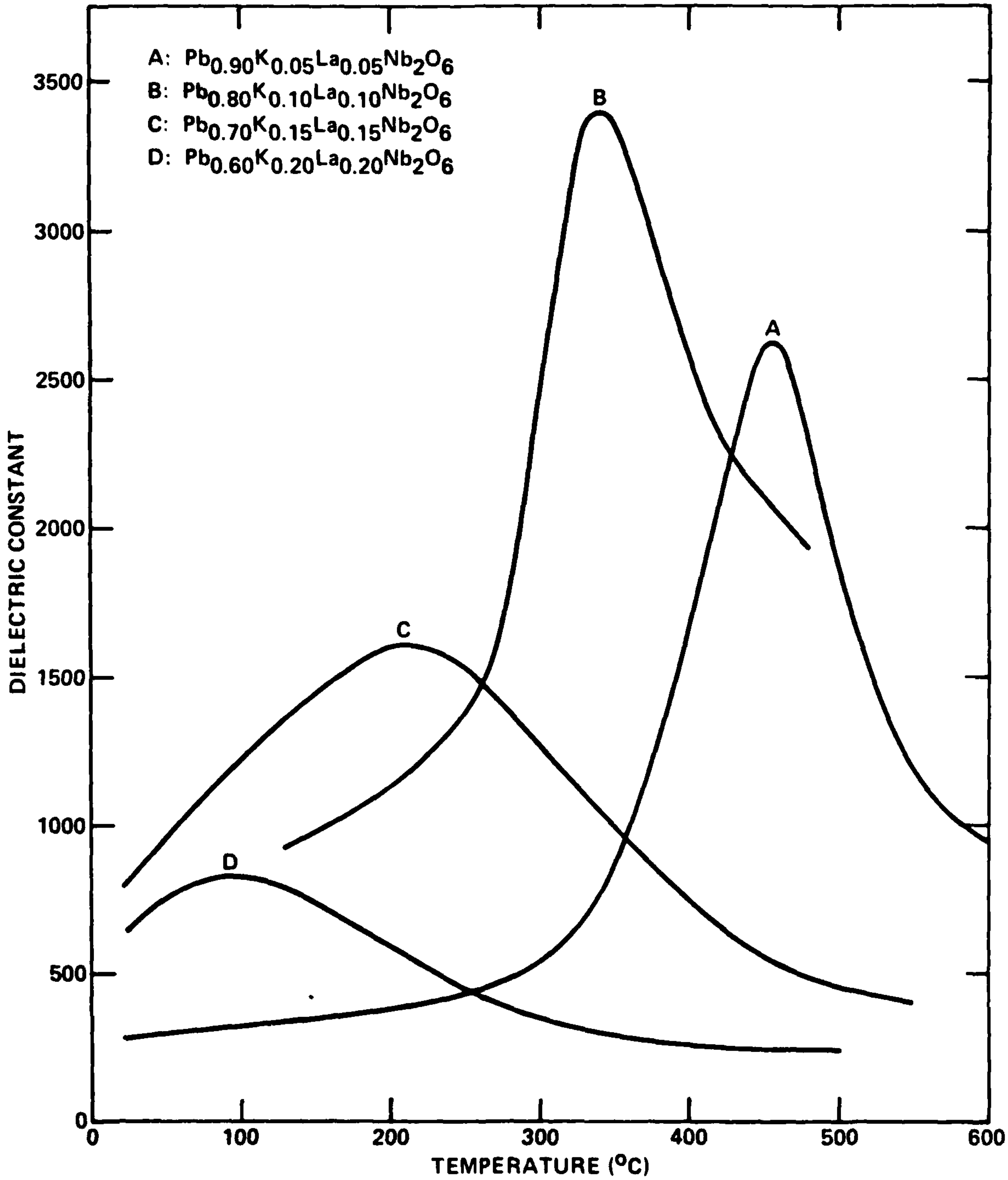
A: $Pb_{0.90}K_{0.05}La_{0.05}Nb_2O_6$
B: $Pb_{0.80}K_{0.10}La_{0.10}Nb_2O_6$
C: $Pb_{0.70}K_{0.15}La_{0.15}Nb_2O_6$
D: $Pb_{0.60}K_{0.20}La_{0.20}Nb_2O_6$
A
B
C
D
DIELECTRIC CONSTANT
0
500
1000
1500
2000
2500
3000
3500
0
100
200
300
400
500
600
TEMPERATURE (°C)

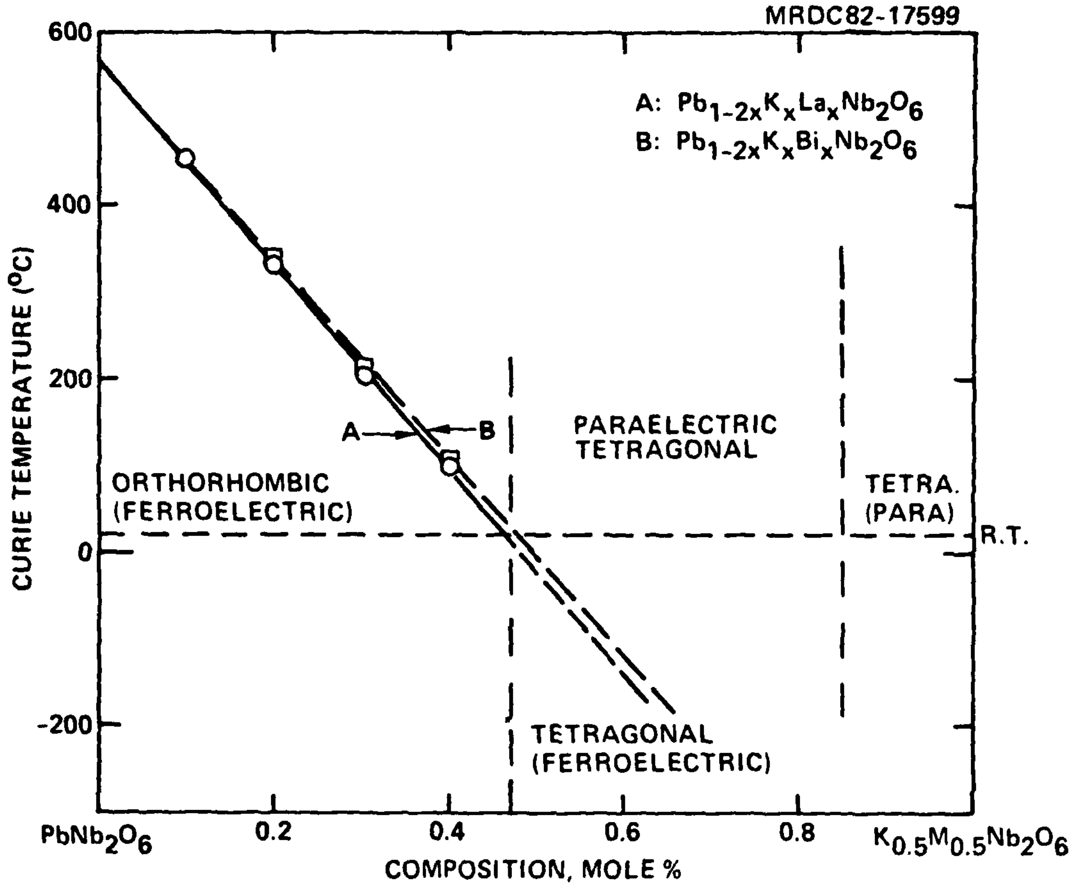
MRDC82-17599
600
400
200
0
-200
CURIE TEMPERATURE (°C)
A: $Pb_{1-2x}K_xLa_xNb_2O_6$
B: $Pb_{1-2x}K_xBi_xNb_2O_6$
A
B
PARAELECTRIC
TETRAGONAL
ORTHORHOMBIC
(FERROELECTRIC)
TETRA.
(PARA)
R.T.
TETRAGONAL
(FERROELECTRIC)
$PbNb_2O_6$
0.2
0.4
0.6
0.8
$K_{0.5}M_{0.5}Nb_2O_6$
COMPOSITION, MOLE %